Quantifying aboveground biomass of Home Covert woodland in the Oxburgh Estate, Norfolk, using Airborne LiDAR.

Home Covert woodland in Oxburgh Estate National Trust property, Oxborough, Norfolk, UK. Image by Amber McDonagh.

Amber McDonagh

Student No: 690037651

Date of submission: 16/09/2024

Word count: 10,106

"I certify that this dissertation is entirely my own work and no part of it has been submitted for a degree or other qualification in this or another institution. I also certify that I have not collected data nor shared data with another candidate at Exeter University or elsewhere without specific authorisation."

Signed: ……

Table of contents

List Of Figures

List Of Tables

Keywords

LiDAR – Light Detection and Ranging

ALS – Airborne Laser Scanning

AGB – Aboveground Biomass

NT – National Trust

GHG – Greenhouse Gas Emissions

DBH – Diameter at Breast Height

DTM – Digital Terrain Model

DSM – Digital Surface Model

CHM – Canopy Height Model

OS – Ordnance Survey

EA – Environment Agency

ITS – Individual Tree Segmentation

GIS – Geographical Information Systems

CRS – Coordinate Reference System

AOI – Area of interest

Abstract

This study evaluates the use of airborne LiDAR data to quantify aboveground biomass (AGB) and carbon storage in Home Covert woodland, a 16-hectare mixed temperate woodland located within the National Trust's Oxburgh Estate, Norfolk, UK. The research compares two LiDAR datasets—publicly available 2018 Environment Agency (EA) data and a 2023 drone-based LiDAR survey commissioned by the National Trust. Using individual tree segmentation (ITS) and allometric equations specific to Palearctic woodland, key metrics such as tree height, crown area, and AGB were extracted. Results indicate that the 2023 drone dataset, with its higher resolution (300+ points/m²), provided significantly more accurate biomass estimates compared to the EA 2018 dataset. The drone survey estimated a **total AGB of 17.8 million kg** and **CO_2 sequestration of 22.26 million kg**, nearly doubling the estimates derived from the 2018 EA data. This research demonstrates the efficacy of high-resolution drone LiDAR in improving biomass and carbon stock assessments, providing valuable insights for woodland management and conservation efforts. By refining LiDAR-based methodologies, this work supports the National Trust's goal of achieving Net Zero carbon by 2030. Additionally, the study highlights the importance of using advanced remote sensing techniques in enhancing precision in woodland monitoring, with broader implications for climate change mitigation and carbon credit systems.

1.0 Introduction

1.1 Importance of Woodlands

Woodlands are integral components of the global carbon cycle, functioning as substantial carbon sinks and playing a critical role in mitigating climate change (Rodríguez-Veiga *et al.*, 2019). Occupying approximately 30% of the Earth's terrestrial surface, forests and woodlands constitute the dominant terrestrial ecosystems (Martone *et al.*, 2018). In Great Britain, these ecosystems sequester approximately 213 million tons of carbon, with projections indicating that this capacity could potentially double as additional carbon is captured (Reid *et al.*, 2021).

Beyond their carbon storage capabilities, woodlands are essential for maintaining biodiversity and preserving vital habitats, contributing significantly to global efforts aimed at reducing atmospheric carbon levels and combating climate change. The terms ‘woodlands’ and ‘forests’ are often used interchangeably, but as described by GOV UK (2024), woodlands are specifically defined as having a minimum area of 0.5 hectares, a minimum width of 20 metres, a tree canopy cover of at least 20%, and a canopy consisting of specimens that meet the definition of trees. Woodlands are characterised by often having high biomass densities, which further enhances their role as carbon sinks.

Despite their ecological importance, the extent of woodland cover in the UK remains limited, underscoring the critical need for targeted conservation and expansion efforts. Woodland cover in the UK comprises only 13.3% of the total land area, approximately 3.21 million hectares of woodland (Reid *et al.*, 2021); a figure substantially lower than the European average of 37% (Hardaker, 2018; FAO, 2015). England, in particular, accounts for merely 1.31 million hectares of woodland, representing just 10% of its total land area (Reid *et al.*, 2021). Given this restricted distribution, the role of UK woodlands in carbon sequestration is increasingly vital, with England alone estimated to store approximately 453.3 million tons of carbon dioxide (CO_2) equivalent, and Great Britain collectively storing around 818.3 million tons (Zellweger *et al.*, 2022). These statistics emphasise the necessity for robust conservation strategies to ensure woodlands remain integral to the UK's environmental objectives.

The global recognition of the importance of forests and woodlands in addressing climate change is evidenced by international commitments to halt deforestation. During the United Nations COP28 climate summit, over 100 world leaders reaffirmed their commitment to ending and reversing deforestation by 2030 (Kumar and Donnelly, 2024). Despite such commitments, UK woodlands face substantial threats from various factors, including rapid urban expansion, invasive species, tree diseases, air pollution, and inadequate tree management practices (Panzavolta *et al.*, 2021; Marzano and Urquhart, 2020; Mitchell *et al.*, 2020; Stevens *et al.*, 2020). These challenges, exacerbated by the pressures of intensive agriculture and urbanisation, have led to a marked decline in both the health and extent of the UK's woodland areas.

In response to these mounting challenges, there is a pressing need to enhance the monitoring and conservation of woodlands to ensure their continued effectiveness as carbon sinks. Accurately assessing the future capacity of woodlands to sequester carbon necessitates the

improvement of monitoring methodologies for aboveground biomass (AGB) and carbon storage, particularly through the application of advanced remote sensing techniques. As the threats to woodlands intensify, the development of effective conservation strategies becomes increasingly crucial to safeguarding these terrestrial ecosystems and maintaining their essential role in climate change mitigation.

1.2 Climate Change and Policy

CO_2 is a major trace gas that significantly impacts global biogeochemical cycles, including the global carbon cycle (Mehmood *et al.*, 2020). Global warming, driven by the increased concentration of CO_2 in the atmosphere (Rodríguez-Veiga *et al.*, 2017), is having catastrophic effects on the Earth system. These include rising sea levels (Frederikse *et al.*, 2020), ocean acidification (Abirami *et al.*, 2021), human displacement due to flooding (Kam *et al.*, 2021), severe storms and weather events (Clarke *et al.*, 2020), loss of biodiversity (Kumar *et al.*, 2021), among many other effects. A key concern addressed within scientific literatures is the depletion of terrestrial carbon storage within forests and woodlands, which plays a critical role in climate change mitigation (Kauppi *et al.*, 2022).

In response to the escalating threat of climate change, countries reaffirmed their commitments under the Paris Agreement at COP28 in 2023, with a focus on reducing emissions and enhancing carbon sequestration through forest protection and tree planting (Araza *et al*., 2023). To monitor national commitments, regular carbon accounting provides essential information, with greenhouse gas (GHG) emissions reported in accordance with the United Nations Framework Convention on Climate Change (UNFCCC) (Hunka *et al.*, 2023). Effective understanding of the global carbon cycle and the success of international economic mechanisms designed to protect and enhance woodland carbon stocks rely heavily on the accurate global monitoring of carbon stored in the AGB of woodlands (Rodríguez-Veiga *et al.*, 2019).

1.3 Aboveground Biomass

Through the process of photosynthesis, carbon is largely stored in trees as aboveground biomass (AGB), which includes all vegetation above ground such as stem, foliage, branches, seeds, and flowers (Rodríguez-Veiga *et al.*, 2017). AGB refers to the total dry mass of living trees found above the ground within a specific plot (Chave *et al.*, 2019), often measured in metric tons of dry matter per hectare (t ha^{-1} or Mg ha^{-1}) or in metric tons of carbon per hectare (t C ha^{-1} of Mg C $ha^{-1)}$ (Rodríguez-Veiga *et al.*, 2017). Quantifying AGB is not only crucial for estimating carbon stocks in UK woodlands but also holds significant social and economic importance, as it provides essential material and energy resources for human use (Rodríguez-Veiga *et al.,* 2019). Additionally, the structure and temporal dynamics of AGB profoundly influence terrestrial ecosystems, directly impacting biodiversity (Pyles *et al.*, 2018), carbon and energy cycles (Houghten *et al*., 2009), and the broader Earth system (Bonan, 2008), which underscores the critical importance of AGB in carbon accounting within the context of a rapidly changing climate. Important to note, changes in AGB are influenced by deforestation and anthropogenic activities, in combination with natural disturbances like

climate variation, which drive annual changes in net primary production (Mäkipää *et al.*, 2008).

To ensure the success of large scale woodland restoration and protection, and the success of previously mentioned climate frameworks and policies, it is crucial to employ accurate and reliable methods for estimating AGB within woodland ecosystems (Jucker *et al.*, 2017). The precision of AGB and carbon quantification is crucial for applications such as greenhouse gas accounting (Araza *et al*., 2023) and initiatives financed through the sale of verified carbon credits (Nonini and Fiala, 2021). However, determining the exact amount of carbon stored in AGB remains challenging due to inconsistencies in measurement techniques, and current Earth observation methods are not fully optimised for precise carbon density quantification (Kellner *et al.*, 2023). Inaccurate estimations of AGB can undermine conservation efforts and result in the misallocation of carbon credits (Demol *et al.*, 2024). Thus, enhancing the accuracy of methods for measuring and monitoring AGB is essential for the integrity of carbon credit systems, as any uncertainty in quantifying these stocks can lead to misinformed policy decisions and the misallocation of funding and resources (Demol *et al.*, 2024).

Direct measurement of AGB is achieved through destructive in situ sampling methods, which involve harvesting and analysing the biomass of trees. While this technique offers high accuracy, it is labour intensive, costly, and impractical for application at larger scales (Rodríguez-Veiga *et al.*, 2017). Moreover, the process is time consuming and limits remeasurement opportunities, making it feasible only for a limited number of trees (Wilkes *et al.*, 2018). As a result, the use of destructive sampling is often restricted to small scale studies or validation of less invasive methods. Due to these limitations, AGB is frequently estimated using non-destructive methods that rely on allometric equations. These equations link easily measurable parameters, such as diameter at breast height (DBH), tree height, and projected crown area, to biomass (Camarretta *et al.*, 2019; Wilkes *et al.*, 2018). By using these relationships, researchers can estimate AGB without the need to harvest trees, making this approach far more feasible for large scale applications.

Forest inventories, which are widely used for AGB monitoring, collect *in situ* measurements of biophysical attributes like DBH, tree height, and plant cover (Cunliffe *et al.*, 2022). These measurements are then applied to allometric models to predict AGB. The accuracy of such estimates can range between 2% and 20%, making them a valuable tool in forestry management and conservation efforts (Rodríguez-Veiga *et al.*, 2017). However, the data derived from these inventories are not always directly comparable across different regions or countries (Rodríguez-Veiga *et al.*, 2019). Variations in national forest definitions, the minimum tree diameter sampled, and plot sizes used in these studies can introduce biases in biomass estimates, complicating efforts to create a consistent global picture of forest carbon stocks (Rodríguez-Veiga *et al.*, 2019; Searle and Chen, 2017; Réjou-Méchain *et al.*, 2014).

Despite these challenges, the use of allometric relationships in AGB estimation has a long history and is a standard practice in forestry operations worldwide (Goetz *et al.*, 2009). These methods are continually refined to improve their accuracy and applicability, reflecting the

ongoing need to enhance our understanding of woodland carbon dynamics. The combination of well documented allometric relationships and forest inventory data provides a robust framework for estimating AGB, though ongoing improvements are necessary to address the inherent limitations and ensure that estimates remain as accurate and reliable as possible.

There exists a plethora of different allometric equations for estimating AGB, ranging from general models (Jucker *et al.*, 2017; Paul *et al.*, 2015) to species-specific equations (McIntire *et al.*, 2022; Rance *et al.*, 2016). Research indicates that species-specific allometric equations yield the most accurate AGB estimates, underscoring the importance of selecting the most appropriate equation for a given context (Pati *et al.*, 2022; Abich *et al.*, 2019). This careful selection is crucial in minimising uncertainty and error in biomass estimations. It is important to recognise that a significant portion of carbon is stored in belowground biomass. In many contemporary approaches, belowground biomass is typically inferred by applying standardized root-to-shoot ratios to AGB values (Paul *et al.*, 2019; Mokany *et al.*, 2006). The scope of this study is limited to AGB estimation and does not encompass other biomass components, such as belowground biomass, soil carbon, or coarse woody debris.

1.4 Airborne LiDAR & its role in AGB estimation

The use of remotely sensed data to model AGB has advanced rapidly in recent years, with increasingly sophisticated models and diverse approaches emerging (Camarretta *et al.*, 2019). Remote sensing offers a powerful means of extending biomass predictions over vast areas, providing unprecedented spatial coverage (Cunliffe *et al.*, 2022). Its ability to capture high resolution, synoptic data at frequent intervals, opens new possibilities for monitoring woodland biomass dynamics with precision (Wilkes *et al.*, 2018). These advancements have already been applied across various scales, leveraging both active and passive sensors from satellite and aerial platforms to enhance AGB estimation and monitoring (Wilkes *et al.*, 2018). A wide range of studies have demonstrated the effectiveness of estimating AGB by enhancing the accuracy of canopy height estimations, improving AGB modelling and biomass predictions in woodland ecosystems using optical data, LiDAR, or a fusion of both techniques (Torres de Almeida *et al.*, 2022; Camarretta *et al.*, 2019).

Airborne LiDAR (Light Detection and Ranging) technology offers significant advancements in quantifying AGB by capturing high resolution, detailed measurements of vertical tree and woodland structures, including canopy height, crown size, and stem density (Wilkes *et al.*, 2018). Airborne LiDAR is an active remote sensing technology that captures the reflected echo and frequency of laser pulses emitted from an aircraft, calculating the difference between the sent signal and the reflected response, which generates a three-dimensional point cloud that precisely represents the vegetation structure within woodlands (Aricak *et al.*, 2023; Chamberlain *et al.*, 2021; Li *et al.*, 2020).

LiDAR sensors can be mounted on various platforms, such as aircraft, satellites, and ground-based systems, providing data at different scales and spatial resolution (Cunliffe *et al.*, 2022; Wilkes *et al.*, 2018). Despite its effectiveness, LiDAR can be limited in capturing fine-scale structural changes in vegetation, and its deployment remains costly in many regions (Cunliffe *et al.*, 2022). Some studies argue that despite its high initial setup costs, LiDAR technology is

a relatively cost effective and rapid method for generating spatial data compared to photogrammetric techniques and terrestrial measurements (Aricak *et al.*, 2023). Spaceborne LiDAR, while offering large scale data collection, faces challenges such as saturation at higher AGB levels, where the signal becomes too weak to penetrate dense canopies and accurately measure AGB (Rodríguez-Veiga *et al.*, 2019; Fagan and DeFries, 2009). To mitigate these limitations, regional studies often calibrate LiDAR-derived algorithms with ground based AGB measurements and airborne LiDAR datasets (Asner et al., 2014; Rodríguez-Veiga *et al.*, 2019). However, even these approaches require substantial *in situ* data to validate the relationship between AGB and LiDAR metrics (Rodríguez-Veiga *et al.*, 2019).

Numerous studies have demonstrated robust correlations between ground based measurements of AGB and those obtained from remote sensing technologies, suggesting that 3D point clouds can accurately capture detailed spatial information at finer resolutions than traditional ground methods (Gleason and Im, 2012). While both methods require allometric models to relate AGB with 3D point clouds and ground data, developing these models can be costly and destructive, with challenges in transferring findings across different study systems (Camarretta *et al.*, 2019). Jucker *et al.* (2017) addressed this challenge by developing global allometric equations for diameter and biomass, which rely on simple RS metrics such as tree height and crown width. Using a large global dataset, this method provides a promising framework for refining AGB estimation despite its general nature, enhancing the accuracy of AGB predictions using relatively simple metrics.

1.5 Individual Tree Detection & Point Cloud Analysis

Modern LiDAR technology has significantly advanced the ability to estimate tree attributes at the individual tree level, largely due to improvements in sampling rates (Zhang *et al.*, 2015; Reitberger *et al.*, 2009; Kwak *et al.*, 2007; Koch *et al.*, 2006; Brandtberg *et al.*, 2003; Persson *et al.*, 2002). A variety of methods have been explored to detect individual trees, many of which rely on a LiDAR-derived canopy height model (CHM), generated through the rasterisation and interpolation of 3D point cloud data (Yang *et al.*, 2020; Zhang *et al.*, 2015). Despite their widespread use, particularly in commercial settings due to the speed of processing and software availability, CHM-based methods have inherent limitations. The generation of CHM using raw point clouds often result in substantial point data loss from multiple levels in the canopy (Tian *et al.,* 2021; Gaulton *et al.*, 2010). The interpolation process and the choice of grid spacing introduce errors and uncertainties, which can further impact the accuracy of tree metric estimations. Additionally, the Gaussian smoothing applied to reduce surface roughness in CHMs can lead to over- or underestimation of tree height (Yu *et al.*, 2023; Adam *et al.*, 2020; Sibona *et al.*, 2017; Zhang *et al.*, 2015).

To overcome the limitations associated with rasterisation and CHM generation, point cloud-based methodologies offer a more accurate approach for individual tree segmentation by directly analysing 3D point clouds. Numerous techniques exist for individual tree detection and segmentation (ITD/ITS) using point cloud data, including voxel-based clustering, K-means clustering, Markov-based clustering, and global clustering methods (Aljumaily *et al.*, 2023; Yang *et al.*, 2020; Morsdorf *et al.*, 2003). One notable method, proposed by Li *et al.*

(2012), segments individual tree crowns based on the relative spacing between trees. Known as the Li2012 algorithm, this approach has been widely adopted in the literature and has demonstrated reliable results for individual tree segmentation (Liu *et al.*, 2023; Roussel *et al.,* 2020). Given its proven efficacy for estimating AGB, this method will be the adopted approach for this project.

1.6 The National Trust

The National Trust (NT), Europe's largest conservation organisation, is responsible for managing an extensive land portfolio exceeding 250,000 hectares across England, Wales, and Northern Ireland. This includes over 26,000 hectares of woodland distributed across 400 properties under active management (National Trust, 2024a). The primary aim of the Trust is the conservation of both heritage sites and natural landscapes, with a focus on ensuring their long term preservation and accessibility for future generations (National Trust, 2024a). A key element of this stewardship involves accurate estimation of woodland AGB, which is essential for effective woodland management and carbon storage assessments.

In alignment with its target to achieve Net Carbon Zero by 2030, the National Trust has committed to the establishment of 20 million new trees, increasing tree coverage from 10% to approximately 17%, consistent with the Climate Change Commission’s goal for the UK (National Trust, 2024b). Accurate quantification of current carbon stocks stored in AGB and the development of robust methodologies to monitor biomass changes due to woodland planting and management are essential to achieving this objective (National Trust, 2024c).

Currently, the Trust employs traditional approaches to estimate woodland AGB, including manual field measurements combined with allometric equations. While these techniques have been widely adopted, they are labour intensive and subject to varying levels of precision. Typically, estimations rely on either a sample of trees within a stand or biomass values extrapolated from species-specific tables, limiting the accuracy and efficiency of the process. To address these limitations, the Trust seeks to explore the potential of remote sensing technologies, such as airborne LiDAR, for improving the accuracy and efficiency of AGB estimation.

This study, conducted in collaboration with the National Trust, evaluates the use of airborne LiDAR technology for enhanced woodland AGB and carbon storage estimation. By integrating both open source and the Trust's commissioned drone LiDAR datasets, this report aims to assess the strengths and limitations of LiDAR-based methods, particularly in terms of their cost effectiveness, time efficiency, and potential to provide more accurate AGB estimation and carbon accounting—contributing to the Trust's broader sustainability and Net Zero objectives.

1.7 Research Project

1.7.1 Study Aim

The primary aim of this project is to evaluate the utility of airborne LiDAR data, sourced from both publicly available datasets and privately commissioned drone surveys, in estimating AGB and carbon storage within the Home Covert woodland stand, part of The National Trust's Oxburgh Estate in Oxborough, Norfolk, UK. The woodland includes a diverse mix of temperate deciduous species and coniferous stands, providing a varied environment for biomass assessment.

This research not only seeks to enhance the precision of AGB estimates for The National Trust but also underscores the importance of accurate allometric models for estimating AGB in conservation management. There is a notable gap in the research concerning differences in AGB results derived from drone-based and satellite-based LiDAR systems, and this project aims to address that by investigating these two distinct data sources. The findings will support The National Trust in refining their methodologies for AGB and carbon storage estimation, advancing their efforts towards sustainable woodland management and their goal of achieving Net Carbon Zero status.

This research utilises Environment Agency airborne LiDAR data from 2018, and drone-based LiDAR data collected by the National Trust in 2023. It focuses on comparing the effectiveness of these two LiDAR platforms, which offer different spatial resolutions, for the assessment of key woodland metrics. Specifically, the study aims to extract tree level information, including tree locations, tree numbers, tree heights, and canopy area, from the LiDAR data. Additionally, it investigates the conversion of these metrics into estimates of AGB and carbon storage of Home Covert. A key focus is on how well the processing of LiDAR point clouds from different datasets can be reproduced and reliably applied across all National Trust properties. This includes evaluating the computational efficiency of the different algorithms employed, taking into consideration of computational time.

1.7.2 Research Questions

1. **Airborne LiDAR utility in Woodand Metrics**
   How effective is airborne LiDAR in determining tree count, height, crown area, and above ground biomass in woodlands?

2. **Carbon Storage**
   What is the aboveground carbon storage this woodland stand, and how confident should we be in this estimate?

3. **Comparison of LiDAR data sources**
   How do drone-derived high resolution LiDAR surveys compare with open source Environment Agency LiDAR in utility for woodland metrics?

2.0 Methodology

2.1 Study Area

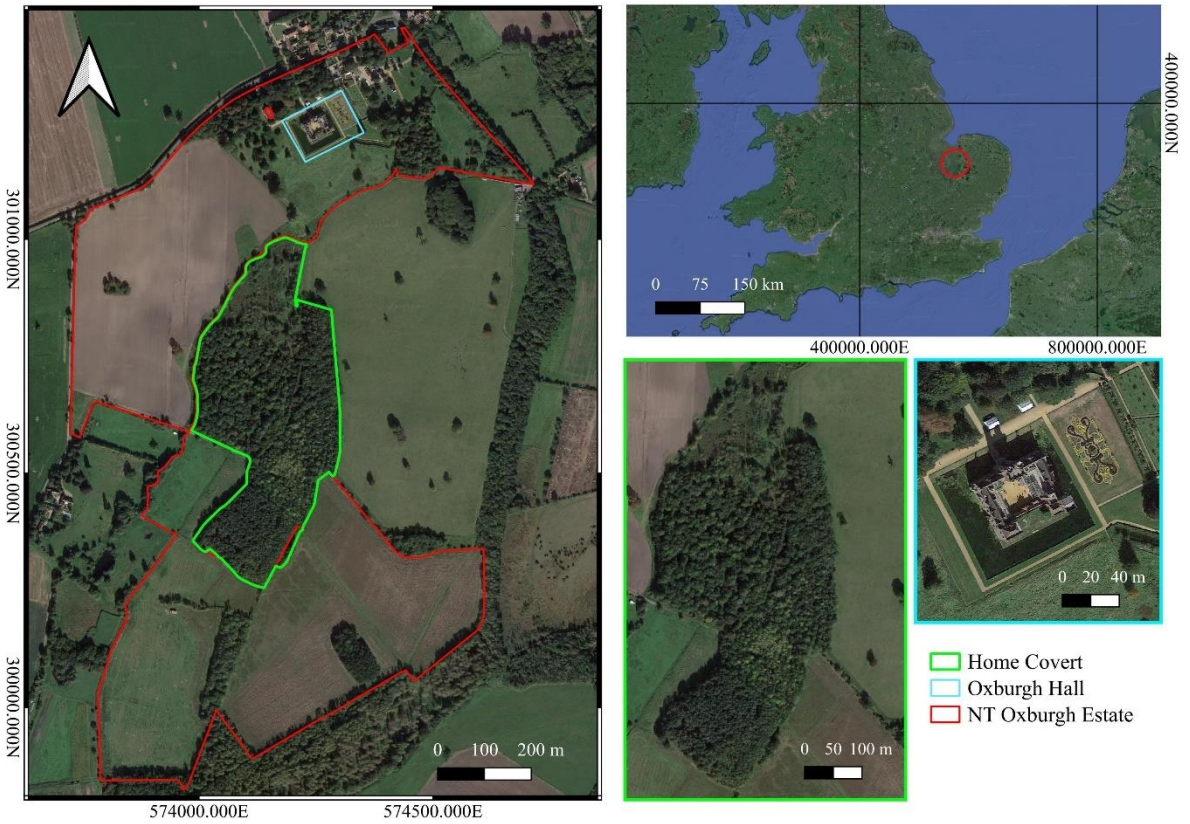

***Figure 1**. Location map of study area of the National Trust Oxburgh Estate in Oxborough, Norfolk, UK, displayed using a Google Satellite basemap. The map highlights Home Covert woodland, Oxburgh Hall and the entire National Trust Oxburgh Estate.*

The focal study area for this research is Home Covert woodland (52° 34' 52" N, 0° 34' 12" E) within the Oxburgh Estate, a National Trust property in Oxborough, Norfolk, UK (**Figure 1**). The woodland spans approximately 0.16 km² (16 hectares).

During an onsite visit to the Oxburgh Estate, a detailed classification of tree species and soil composition within Home Covert was conducted with the assistance of the lead estate ranger, Thomas Day. Home Covert is characterised as a mixed temperate woodland, with its northern section dominated by native deciduous species, including ash (*Fraxinus excelsior*), wild cherry (*Prunus avium*), oak (*Quercus robur*), hornbeam (*Carpinus betulus*), bird cherry (*Prunus padus*), hazel (*Corylus avellana*), field maple (*Acer campestre*), hawthorn

(*Crataegus monogyna*), and blackthorn (*Prunus spinosa*). These species thrive in the wet, sandy, and clay rich soils found throughout the woodland.

***Figure 2**. Basemap comparison of Home Covert woodland at Oxburgh Estate in Oxborough, Norfolk, UK. A) Google Satellite Imagery and b) ESRI Satellite Imagery. The figure highlights the pine planation felling in south region of Home Covert during 2023.*

The southern section of Home Covert comprises a pine plantation, which has recently undergone felling operations in early 2023 (**Figure 2**). Information from the Estate's display boards (**Figure 3**) read that this plantation, originally established under a grant in the 1970s, was present when the National Trust acquired the land in 1989. The pine trees, a non-native coniferous species, were cultivated as a timber crop and had reached maturity, making it the optimal time for harvesting. Following the removal of the pines, surveys by the Oxburgh Estate's Ranger team revealed that this section of Home Covert supports 50% less wildlife compared to other National Trust-managed woodlands (BBC News, 2023). To address this, the 2.7 hectares will be replanted over the next few years with approximately 2,300 native trees, including species such as oak (*Quercus robur*), rowan (*Sorbus aucuparia*), hazel (*Corylus avellana*), hornbeam (*Carpinus betulus*), and field maple (*Acer campestre*). As the replanted woodland matures, it is expected to absorb and store an estimated 1,500 tonnes of CO_2, contributing to the National Trust's carbon sequestration efforts.

Deciduous trees in this region are characterised by their broad leaves, which they shed annually, while coniferous species, which are less prevalent in Home Covert, retain their needle-like or scale-like foliage year round. Nationally, the UK's woodlands are

approximately split between broadleaf (49%) and coniferous (51%) species, though the distribution varies across the UK (Reid *et al.,* 2021).

Figure 3*. Pine Plantation Felling information board within Home Covert woodland at Oxburgh Estate in Oxborough, Norfolk, UK.*

2.2 Data Acquisition

The data sources utilised in this study are presented in **Table 1,** with links provided in **Section 6.0 (Open Research)** at the conclusion of this report. These sources include the Environment Agency (EA) LiDAR 2018 point cloud, which serves as the primary dataset for this research. However, the National Trust drone-based LiDAR 2023 point cloud and Emapsite data are not accessible due to its private commissioning and ownership by the National Trust (NT).

Table 1. Sources of data used to conduct study's research, and their characteristics.

Data	Date	Format	Spatial Resolution	Sources	Usage
National LiDAR Programme Point Cloud	2018	LAZ	1 m (8 points/m^2)	Environment Agency Defra Survey Data - Tile TF70sw	Used to conduct point cloud analysis and extract tree metrics/AGB estimations.
National Trust Drone-based LiDAR Point Cloud	2023	LAS	2-5 cm (300+ points/m^2)	National Trust Oxburgh Estate	Used to conduct point cloud analysis and extract tree metrics/AGB estimations.
National Trust Drone-based LiDAR Photogrammetry	2023	GeoTiff	2-5 cm	National Trust Oxburgh Estate	Display the orthomosaic of Home Covert for visual representation of study area in report.
National Trust Habitats GB	2024	Shapefile	n/a	Emapsite	Habitat and topographic data for Home Covert, used in generation of AOI shapefile.

The 2018 LiDAR point cloud data, provided by the Environment Agency via the Defra Data Download platform, offers precise elevation measurements at a 1 metre spatial resolution. For this study, the dataset corresponding to the Ordnance Survey grid tile TF70sw was specifically downloaded. The discrete LiDAR returns are automatically classified into ground and various vegetation categories, enabling the generation of surface models such as Digital Terrain Models (DTMs) and Digital Surface Models (DSMs). Additionally, the data can be used for further point cloud analyses. The EA employs LiDAR data collection methods that achieve a density of approximately eight points per square metre, providing sufficient detail to capture intricate terrain and vegetation features.

To obtain GIS data for National Trust properties, an account was established with Emapsite, enabling self-service downloads through a contractual agreement (Emapsite, 2024). This collaboration provided access to proprietary habitat and topographic data from the National Trust, facilitating precise boundary delineation of the Home Covert woodland area. The data was integrated into the analysis to generate an exact shapefile of the Home Covert area.

2.2.1 Drone Flight Specifications

Another key dataset utilised in this study was a privately commissioned drone-based LiDAR point cloud dataset acquired in 2023 by the National Trust; LiDAR product with 2-5 cm spatial resolution. This dataset was collected using a DJI M300 RTK drone equipped with a DJI Zenmuse L1 LiDAR sensor. The survey was conducted at an altitude of 70–75 metres above ground level, with a 50% side-lap. The L1 LiDAR sensor was configured to capture the maximum of three returns per pulse. This drone survey produced both a LiDAR point cloud and photogrammetry data, which were used to generate an orthomosaic and a Digital Terrain Model (DTM) and a Digital Surface Model (DSM). A preliminary GIS analysis estimated the point density of the drone dataset to be over 300 points/m². This indicates a highly detailed and high resolution dataset, ideal for capturing fine-scale structural information within the surveyed area.

2.3 Data analysis

The methodology selected for this study is point cloud-based analysis, utilising high resolution data produced by LiDAR technology. This approach retains the full detail of the original LiDAR data, which is often significantly reduced when converted into two-dimensional raster formats, potentially overlooking critical aspects of spatial structure and variability within the scanned area.

Point cloud-based analysis enables a more detailed examination of this high resolution data by analysing reflections within voxels (three-dimensional pixels), offering deeper insights into the density and spatial arrangement of vegetation. This method is particularly well suited for complex environments such as woodlands, where understanding the distribution of vegetation is crucial. Compared to rasterised data, which often simplifies the original information, point cloud analysis maintains the fine spatial resolution and provides enhanced structural insights.

Given that the study area is a relatively small woodland of 16 hectares (40 acre or 0.16 km^2), the individual tree segmentation (ITS) approach was selected. This method allows for a more accurate and representative estimation of AGB on a per-tree basis, enabling detailed analysis at the individual tree level.

2.3.1 Software

To enhance the reproducibility of this project, Free and Open Source Software (FOSS) was utilised throughout the study. FOSS solutions leverage the benefits of community-driven development, promoting the reuse of workflows in future projects both by the National Trust and the broader industry (Fortunato and Galassi, 2021). This approach fosters knowledge sharing and resource accessibility, facilitating the efficient transfer of methodologies, tools and repositories across different projects and users, particularly through platforms such as GitHub (Explore GitHub, 2024). All modelling and analysis were conducted using R

Statistical Software (v4.4.1, R Core Team, 2022). Geographical information systems (GIS) such as QGIS were also used for geovisualisation of results and map generation.

2.4 Workflow

An extensive R script was developed for the methodology, which was applied to both the Environment Agency's 2018 LiDAR point cloud (1 m resolution/ 8 point/m^2) and the National Trust's 2023 drone-based LiDAR point cloud (2–5 cm resolution/ 300+ point/m^2). Minor modifications to the script were made to account for differences in the size of the point clouds. The R scripts can be accessed via the GitHub repository link provided in **Section 6.0 (Open Research)** at the conclusion of this report. The overall methodological approach used to model and map canopy height, tree numbers, crown area, and AGB in Home Covert, based on the two LiDAR datasets, is depicted in **Figure 4**. This research, including its ethics and risk assessment, was approved by project supervisor Andrew Cunliffe and academic tutor Steven Palmer.

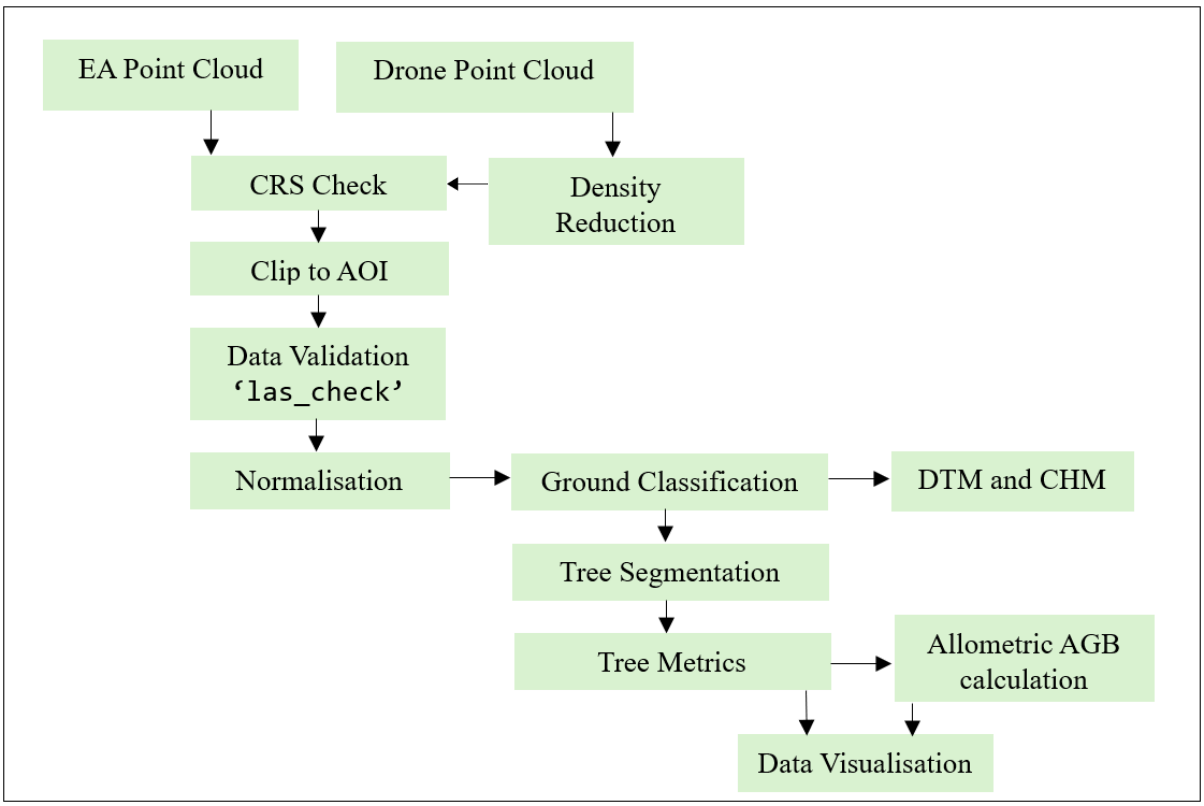

Figure 4. *A designed framework for conducting point cloud analysis on LiDAR datasets to extract tree metrics (e.g. tree height, crown area), AGB estimations and visualise results using R Statistical software.*

2.4.1 Workflow explained

The study commenced with the acquisition of relevant datasets, including point clouds and shapefiles from various sources. These included the EA 2018 LiDAR point clouds, the NT 2023 drone-based LiDAR point cloud, and topographic shapefiles from Emapsite for the area of interest (AOI). For data preparation, essential libraries and packages, particularly the lidR package, were installed into R Studio (specific R Statistical Software used). The data were imported into R, and the shapefile for Home Covert was loaded. The Coordinate Reference

System (CRS) of the shapefile was verified and, if necessary, reprojected to align with the CRS of the point cloud data.

The point cloud data were then clipped based on the AOI, categorising the data into whole woodland coverage, deciduous areas, and coniferous areas. The validity of the clipped data was assessed using summary statistics and visualisations with functions such as `las_check` and `plot`. Data processing included height normalisation of the point cloud using the `knnidw()` function, which avoided rasterisation. Ground points were classified to ensure accurate zero elevation, and negative outliers with Z-values below zero were removed.

Subsequently, Digital Terrain Models (DTMs) and Canopy Height Models (CHMs) were generated to facilitate visualisation of terrain and canopy structures. Individual tree segmentation (ITS) was performed using the `segment_trees` function with parameters from the Li2012 algorithm. This process identified individual trees and calculated crown metrics using the `crown_metrics` function, which provided crown hulls and exported tree crowns as polygons. Additional metrics, including maximum tree height, crown area, perimeter, and crown diameter, were calculated with the `sf` package. For coniferous woodlands, a density reduction of 0.5 was applied to address the high point density, and the parameters '*dt1*' and '*dt2*' for the Li2012 algorithm were adjusted to 0.5 and 1, respectively.

AGB was calculated for coniferous and deciduous trees, as well as for the entire woodland, using selected AGB allometric equations. The AGB values and total biomass were saved in CSV files for further analysis. Carbon estimation calculations were then performed based on the AGB data to assess carbon storage within the study area. Finally, data visualisation and analysis involved creating scatter plots and violin plots to compare AGB with tree height and crown diameter for both coniferous and deciduous trees, focusing on these primary variables for determining AGB.

The primary adjustment in the drone-based methodology involved reducing the point cloud density at the initial stage. To address computational limitations and prevent crashes in R, the point cloud was randomly resampled to reduce its density by 80%, as the original dataset was too large to process and visualise effectively. Previous attempts to reduce the density by 70% and 50% were insufficient in alleviating these issues. The drone-based methodology also did not involve dividing the woodland into deciduous and coniferous areas, as the drone survey was conducted after the felling of the pine plantation in the southern section of Home Covert.

2.4.2 AGB Calculations

Biomass calculations are a powerful tool for estimating AGB, which is essential for assessing carbon storage in vegetation and terrestrial ecosystems. Allometry, the relationship between tree size and biomass, is influenced by factors such as climate, vegetation structure, species, and growth form, leading to variations across woodland biomes and even within regions (Rodríguez-Veiga *et al.*, 2017). Therefore, selecting appropriate allometric equations is crucial, as an unsuitable model can introduce significant errors in AGB estimation.

There is a wide array of allometric equations for AGB estimation, ranging from general models (e.g., Jucker *et al.*, 2017; Paul *et al.*, 2015) to species-specific ones (McIntire *et al.*, 2022; Rance *et al.*, 2016). Research indicates that species-specific equations provide the most accurate AGB estimates, highlighting the importance of selecting the right model to minimise

uncertainty and error (Pati *et al.*, 2022; Abich *et al.*, 2019). However, implementing species-specific equations requires a more complex workflow, including detailed tree classification, which is beyond the scope of this project.

Airborne LiDAR typically cannot reliably measure DBH due to the limited number of returns collected beneath the canopy, preventing accurate reconstruction of trunk morphology. To address this, Jucker *et al.* (2017) developed widely used allometric models that estimate AGB based on crown area and tree height derived from airborne LiDAR. Their research, involving data from over 100,000 trees across diverse forests globally, found a strong correlation between AGB, tree height, and crown diameter. While these models generally provide reliable AGB estimates for different tree and forest types, accuracy improves when adjusted for biome-specific variations in crown architecture and wood density, especially between angiosperms (deciduous) and gymnosperms (coniferous). Jucker *et al.* (2017) offer regional parameters for Palearctic coniferous and deciduous mixed woodlands, suggesting that these group-specific algorithms can be applied with minimal field data, yielding reliable AGB estimates.

A more general allometric equation (**Equation 1**) was initially applied to estimate the AGB of the entire woodland of Home Covert. This equation was adapted from models proposed by Wilkes *et al.* (2018), Aabeyir *et al.* (2022), and Muumbe *et al.* (2024), which incorporate various allometric relationships based on tree height, diameter, and crown dimensions. Additionally, it integrates temperate woodland-specific models, particularly for mixed broadleaf and coniferous forests, as outlined by Jenkins *et al.* (2003), Chave *et al.* (2005), Zianis et al. (2005), and Jucker et al. (2017).

Although this equation was eventually excluded from the final analysis due to its overly general nature, it is included in the report for its utility in providing an initial estimate of AGB for the entire woodland.

The generalised allometric equation for temperate mixed deciduous and coniferous woodland AGB is as follows:

Equation 1

$$\mathbf{AGB = \beta0 + \beta1 * \log(TreeHeight) + \beta2 * \log(CrownArea) + \beta3 * \log(CrownPerimeter)}$$

The best fit AGB model from Jucker *et al.* (2017):

Equation 2

$$AGB_{pred} = (0.016 + \alpha_G) \times (H \times CD)^{(2.013+\beta G)} \times \exp[0.204^2/2]$$

where α_G and β_G are functional group-dependent parameters which represent the difference in the scaling constant α and scaling exponent β between angiosperm and gymnosperm trees. For gymnosperms, $\alpha_G = 0.093$ and $\beta_G = -0.223$, whereas for angiosperms both parameters are set to zero.

2.4.3 Carbon Storage

The carbon content in wood (C) varies by species, but it is generally estimated to constitute 47% of the dry weight of the tree's wood component (Chave *et al.*, 2019). This 47% biomass-to-carbon ratio has been widely used in studies of carbon content in biomass (Fawcett *et al.*, 2022; Chave *et al.*, 2019). The dry weight of wood is typically around 72.5% of the green (fresh) weight, or AGB, according to previous research (Hanif *et al.*, 2015; DeWald *et al.*, 2005; Birdsey, 1992).

Thus, the carbon content of a tree can be estimated using the following equation:

$$\mathbf{C = AGB \times 0.725 \times 0.47C}$$

This equation first calculates the dry weight of the tree, followed by multiplying it by 47% to determine the carbon content.

The amount of CO_2 stored in a tree, corresponding to its carbon content, varies significantly depending on species, growth conditions, and woodland management practices. However, it is commonly estimated using a factor of 3.67 × C, which reflects the ratio of carbon to oxygen atoms in CO_2. This factor allows for the conversion of stored carbon (C) into the equivalent amount of sequestered CO_2 (Hanif *et al.*, 2015; DeWald *et al.*, 2005; Birdsey, 1992).

2.4.4 Ground Data

Incorporating UK tree allometry with ground data facilitates the comparison of AGB estimation accuracy across different LiDAR datasets. However, obtaining sufficient ground data for a comprehensive analysis was beyond the scope of this study. Instead, ten random tree measurements were collected at Home Covert to provide a preliminary comparison.

Fieldwork was conducted on 16th July 2024 within Home Covert, located at the National Trust's Oxburgh Estate in Norfolk. Ten random locations were selected within the woodland, with accessibility considerations for the terrain. An exploratory survey of the area was carried out to sample the species composition, aided by the PlantNet tree identification app. The detected trees were all deciduous and belonged to various species families, including Betulaceae, Fagaceae, Ulmaceae, and Sapindaceae. The specific tree species identified were *Carpinus betulus* L. (European hornbeam, Betulaceae), *Quercus robur* L. (Common oak, Fagaceae), *Acer campestre* L. (Field maple, Sapindaceae), *Ulmus* × *hollandica* Mill. (Dutch elm, Ulmaceae), *Acer rubrum* L. (Red maple, Sapindaceae), *Fagus sylvatica* L. (Beech, Fagaceae), and *Quercus petraea* (Matt.) Liebl. (Sessile oak, Fagaceae).

Tree measurements were obtained using a Suunto PM-5 Clinometer, a 150 cm double-sided tape measure, a 30 m tape measure, and a GPS receiver. The methodology involved measuring tree height using a clinometer, using tape measures to record diameter at breast height, and capturing geolocation with a GPS receiver. Tree height was calculated using trigonometry.

2.5 Possible Limitations

AGB is generally estimated rather than directly measured, which introduces substantial uncertainties (Clark and Kellner, 2012). These uncertainties stem from factors such as tree height estimation, wood density, and the selection of allometric models, with individual tree-level AGB estimates potentially having an absolute error of approximately 50% (Chave *et al.*, 2014; Chave *et al.*, 2019). The use of generalised allometric functions in LiDAR-based biomass analysis offers advantages in terms of speed, as it bypasses the need for tree classification. However, this comes at the expense of accuracy and specificity, as general models may not account for the variability between different tree species and woodland types. It is important to acknowledge that the use of generalised allometric equations, combined with the absence of extensive ground data, introduces a degree of uncertainty and potential error in the accuracy of AGB estimations. This limitation should be considered when interpreting the results and conclusions of this study.

3.0 Results

Table 2. Allometric values for Palearctic woodland types (Jucker *et al.*, 2017).

Biogeographic region	Forest type	Functional group	α	β
Palearctic	Temperate coniferous forests	Gymnosperm	0.093	-0.223
Palearctic	Temperate mixed forests	Angiosperm	0	0

Table 3. Tree metric values for 2018 EA LiDAR point cloud.

Woodland type	No. Trees (max height)	Max tree height (m)	Avg Tree Height (m)	Max crown area (m^2)	Avg Crown Area (m^2)	Max crown perimeter (m)	Max Crown diameter (hull) (m)	Avg Crown Diameter (hull) ($m^)$
Temperate coniferous	3693	24.07	8.895	99.89	2.38	43.41	43.41	6.11
Temperate deciduous	17749	28.84	11.13	144.82	3.92	47.29	47.29	7.11
Whole woodland	19789	28.84	11.544	161.76	4.92	51.06	51.06	7.67

Table 4. Tree metric estimates for 2018 EA LiDAR point cloud using Jucker *et al.* (2017).

Woodland type	Average AGB per tree (kg)	Total AGB (kg/ha)	Total C (kg/ha)	Total CO2 sequestered (kg/ha)
Temperate coniferous forests	220.09	812,784.33	276,956.26	1,016,429.47
Temperate deciduous forests	309.59	442,468.54	150,771.16	553,330.16
Whole temperate forest	292.81	511,840.19	174,409.54	640,083.03

Table 4 presents key metrics, including average AGB per tree (kg), total AGB (kg/ha), total carbon content (kg/ha), and total CO_2 sequestered (kg/ha). Using these values, the total AGB for Home Covert, covering 16 hectares, is estimated at **8,189,443.04 kg**, total carbon content is **2,790,552.72 kg** and a predicted total of **10,241,328.47 kg** of CO_2 sequestered within Home Covert (**Table 7**). These calculations are derived from the 2018 EA LiDAR dataset.

Table 5. Tree metric values for NT Drone data.

Woodland type	No. Trees	Max tree height (m)	Average Tree Height (m)	Max crown area (m^2)	Average Crown Area (m^2)	Max crown perimeter (m)	Max Crown diameter (hull) (m)	Ave Crown Diameter (hull) ($m^)$
Whole temperate deciduous woodland	10,577	39.78	11.83	312.97	20.42	67.74	62.74	15.09

Table 6. Tree metric estimates for NT Drone point cloud using Jucker *et al.* (2017).

Woodland type	Average AGB per tree (kg)	Total AGB (kg/ha)	Total C (kg/ha)	Total CO2 sequestered (kg/ha)
Whole temperate deciduous woodland	1678.94	1,112,525.75	379,093.15	1,391,271.86

Table 6 presents key metrics, including average AGB per tree (kg), total AGB (kg/ha), total carbon content (kg/ha), and total CO_2 sequestered (kg/ha) of whole Home Covert study area. Using these values, the total AGB for Home Covert, covering 16 hectares, is estimated at **17,800,412 kg**, total carbon content is **6,065,490.39 kg** and a predicted total of **22,260,349.73 kg** of CO_2 sequestered within Home Covert (**Table 7**). These calculations are derived from the 2023 NT drone-based LiDAR dataset.

Table 7. AGB, C and CO_2 values for whole area of Home Covert for 2018 EA LiDAR point cloud and 2023 Drone point cloud, using Jucker *et al.* (2017) allometric equations.

LiDAR dataset	Woodland type	Average AGB per tree (kg)	Total AGB (kg)	Total C (kg)	Total CO2 sequestered (kg)
EA 2018	Whole temperate deciduous woodland	292.81	8,189,443.04	2,790,552.72	10,241,328.47
Drone 2023	Whole temperate deciduous woodland	1678.94	17,800,412	6,065,490.39	22,260,349.73

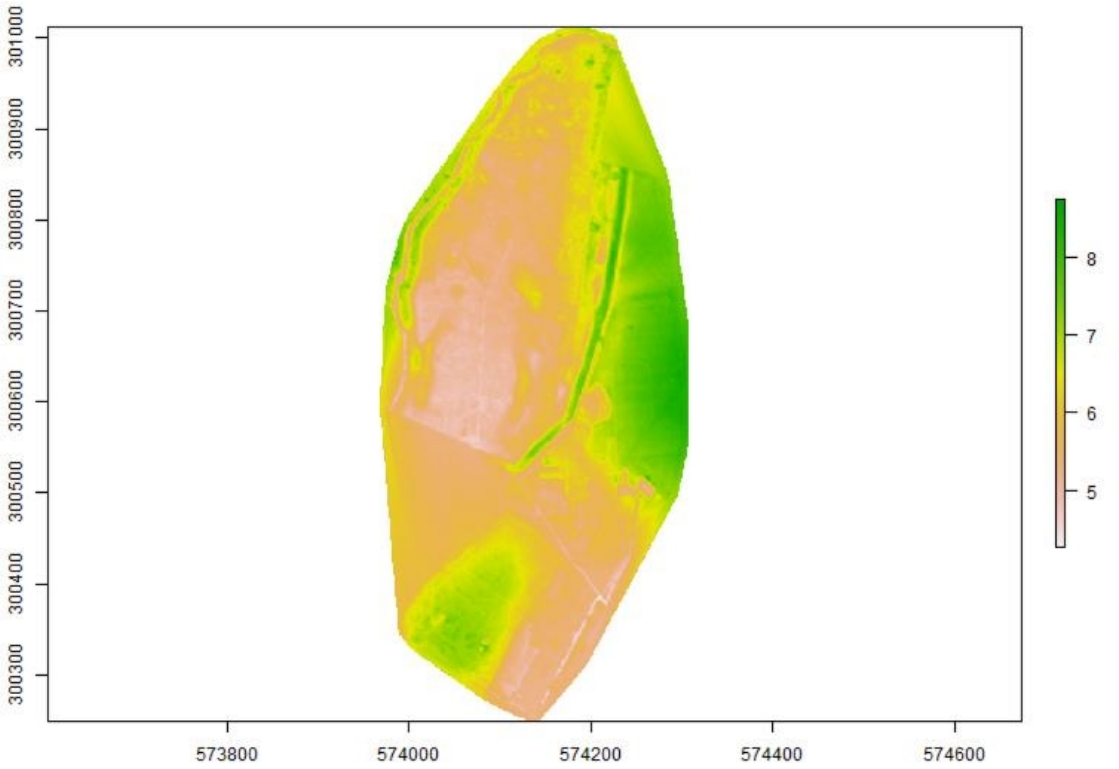

Figure 5. *Digital Terrain Model (DTM) of Home Covert woodland.*

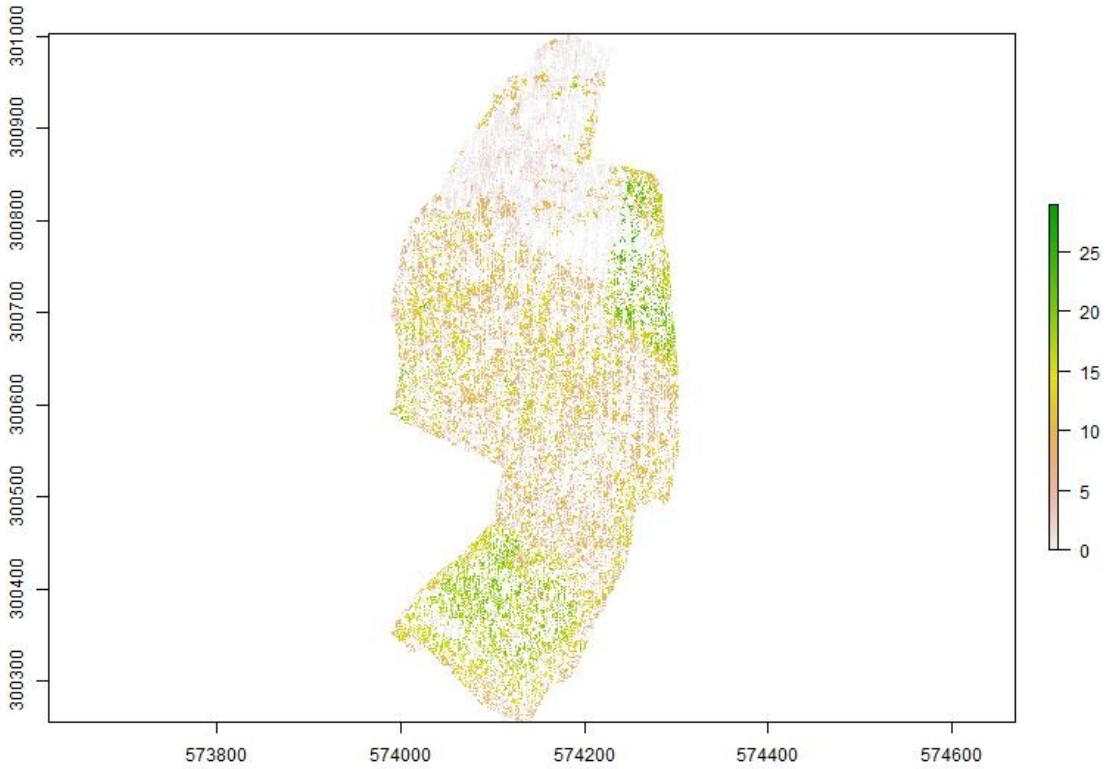

Figure 6*. Canopy Height Model (CHM) of Home Covert woodland using Environment Agency 2018 point cloud data. Scale represents tree height (m).*

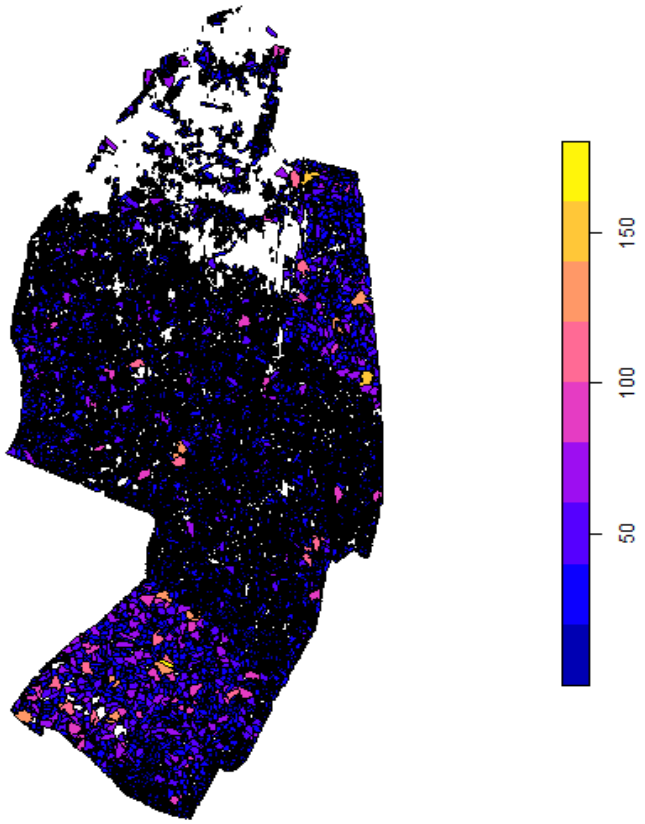

***Figure 7**. Tree crown area (convex hull) of Home Covert woodland as polygons using Environment Agency 2018 point cloud data. Scale represents crown area (m^2).*

***Figure 8**. Relationship between above ground biomass and the product of maximum tree height and crown diameter, in coniferous (gymnosperm) and deciduous (angiosperm) trees, using 2018 EA LiDAR point cloud.*

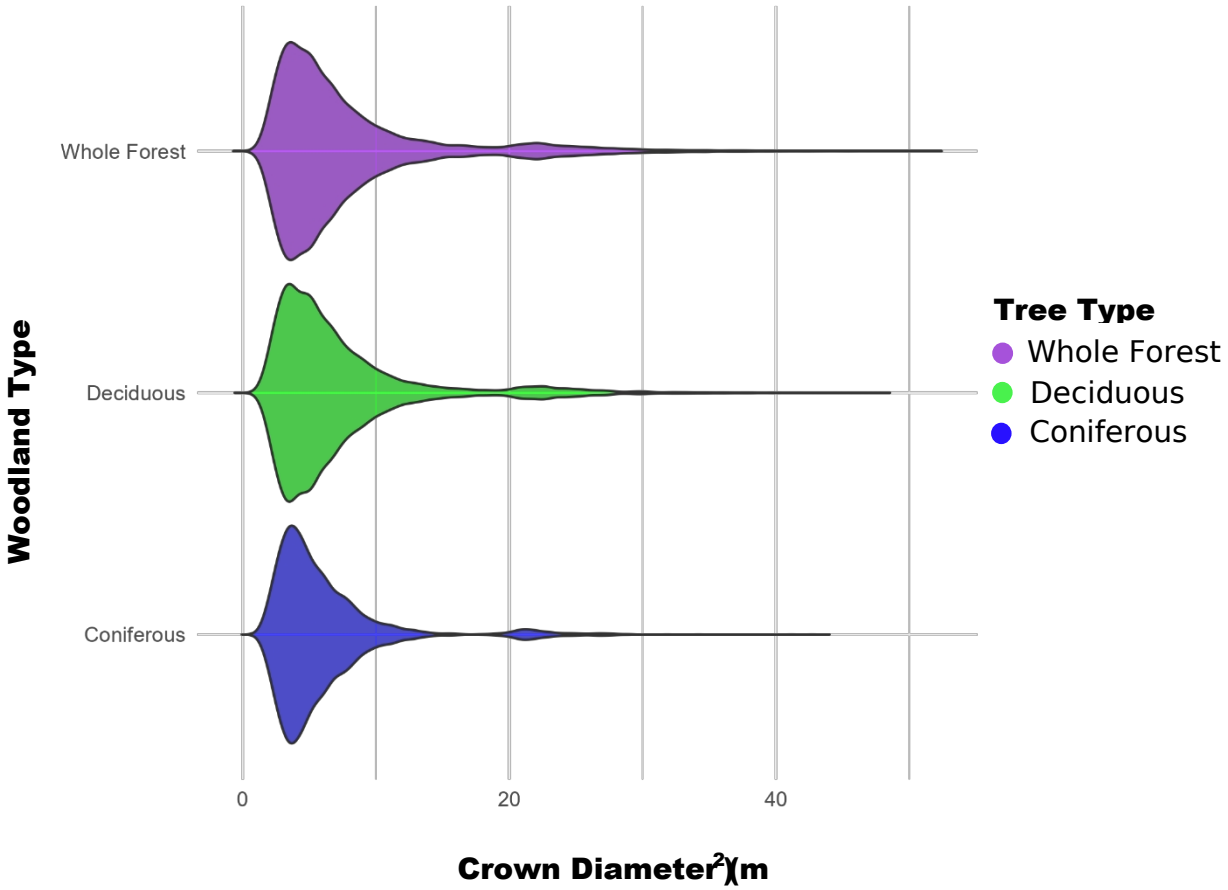

Figure 9. *Violin plot showing tree size distribution (by tree crown diameter), categorised by woodland type within Home Covert, using 2018 EA LiDAR point cloud.*

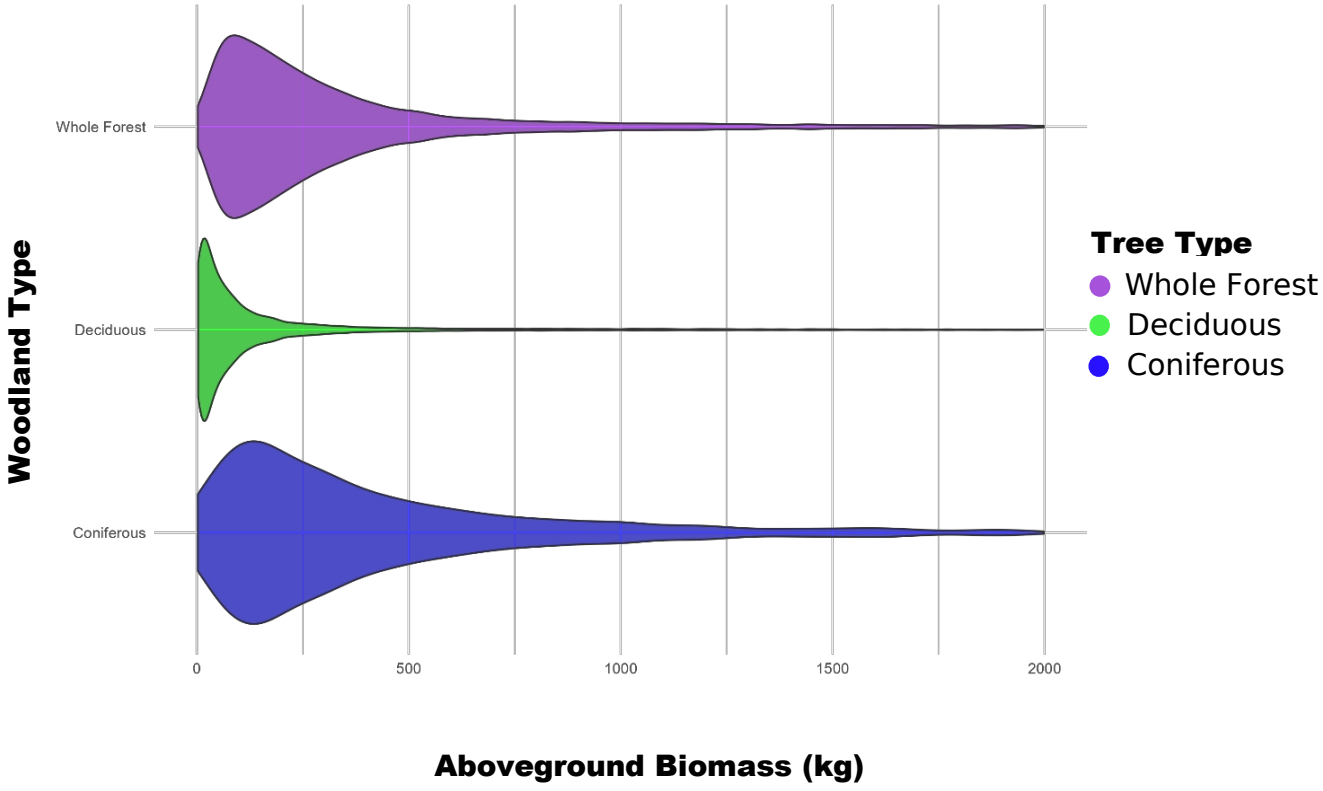

Figure 10. *Violin plot showing tree size distribution (by AGB), categorised by woodland type within Home Covert, using 2018 EA LiDAR point cloud.*

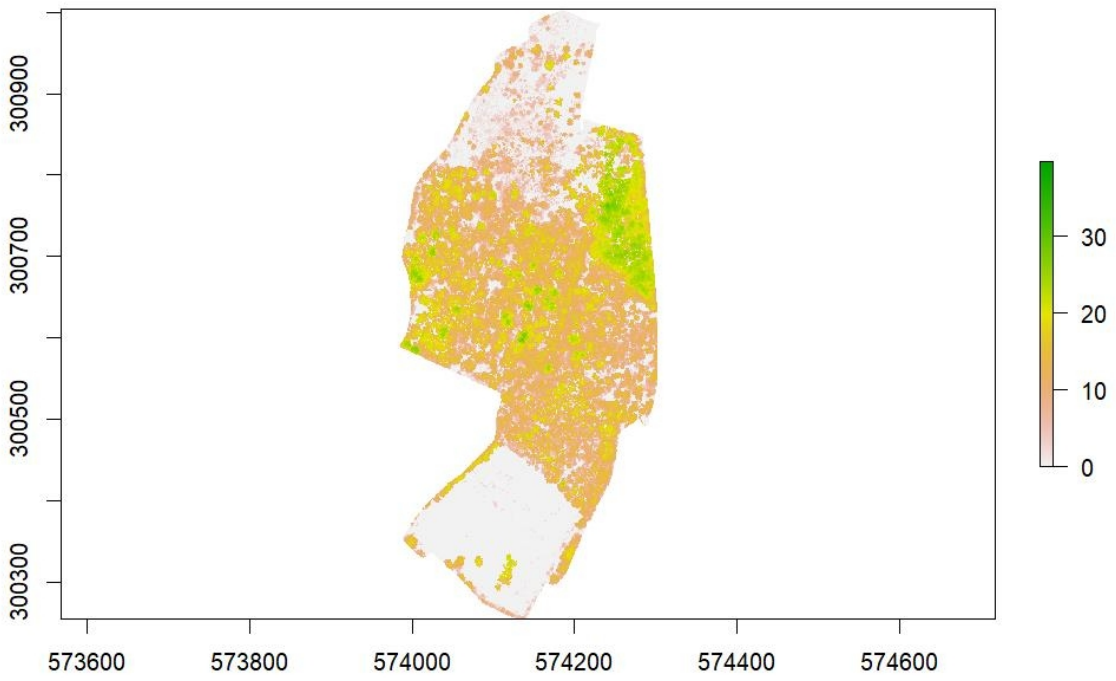

Figure 11. *Canopy Height Model (CHM) of Home Covert woodland using drone point cloud data. Scale represents tree height (m).*

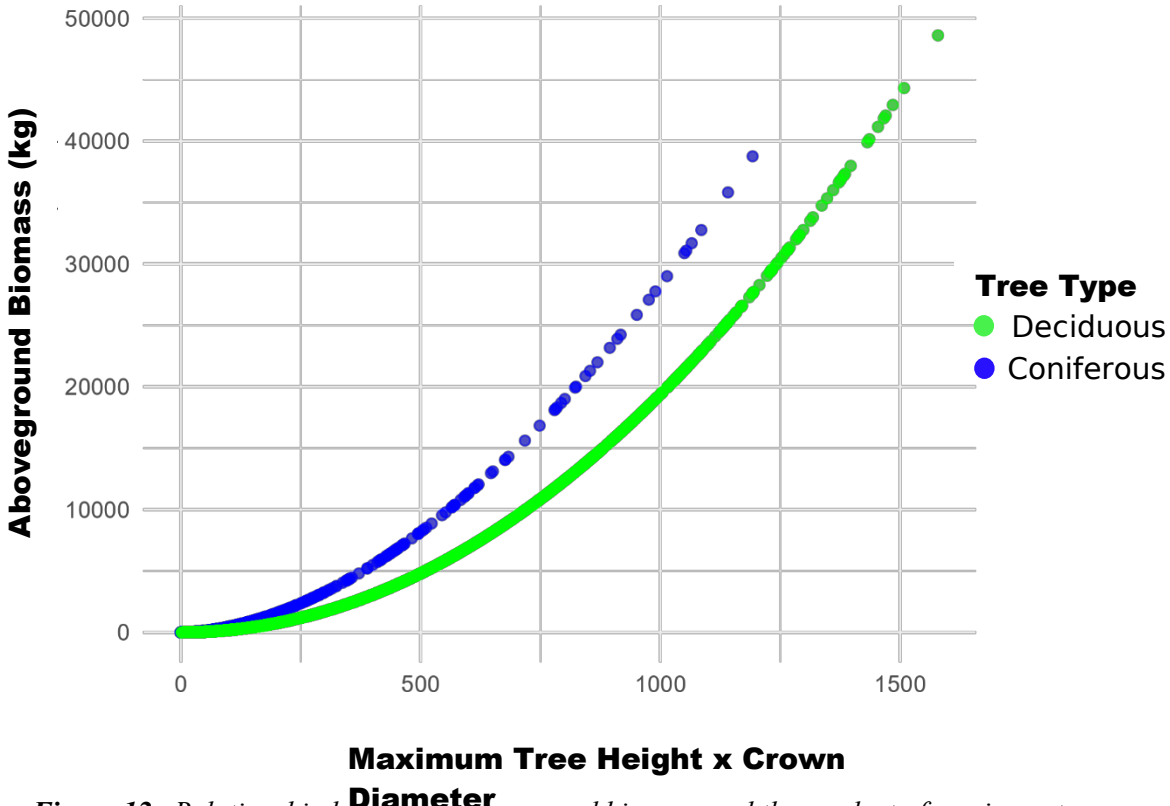

Figure 12. *Relationship between above ground biomass and the product of maximum tree height and crown diameter, in coniferous (gymnosperm) and deciduous (angiosperm) trees, using 2023 drone point cloud.*

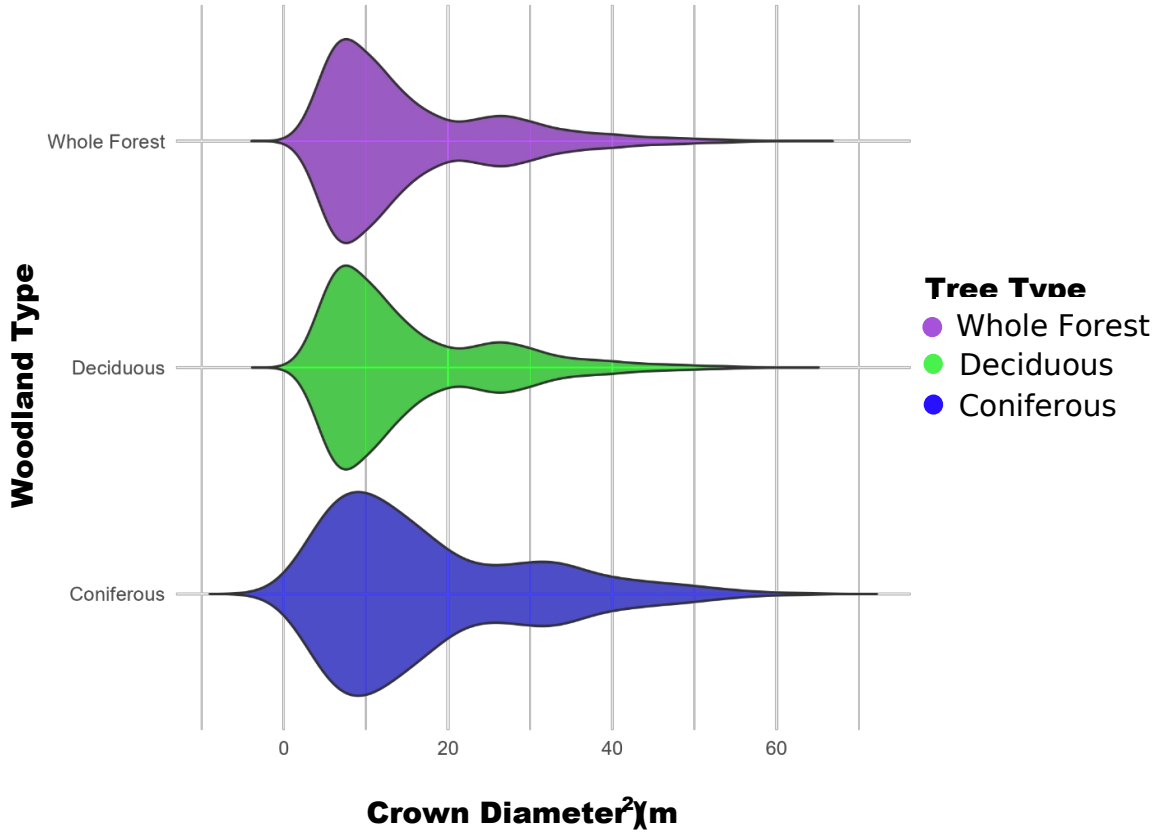

Figure 13. *Violin plot showing tree size distribution (by tree crown diameter), categorised by woodland type within Home Covert, using 2023 drone point cloud.*

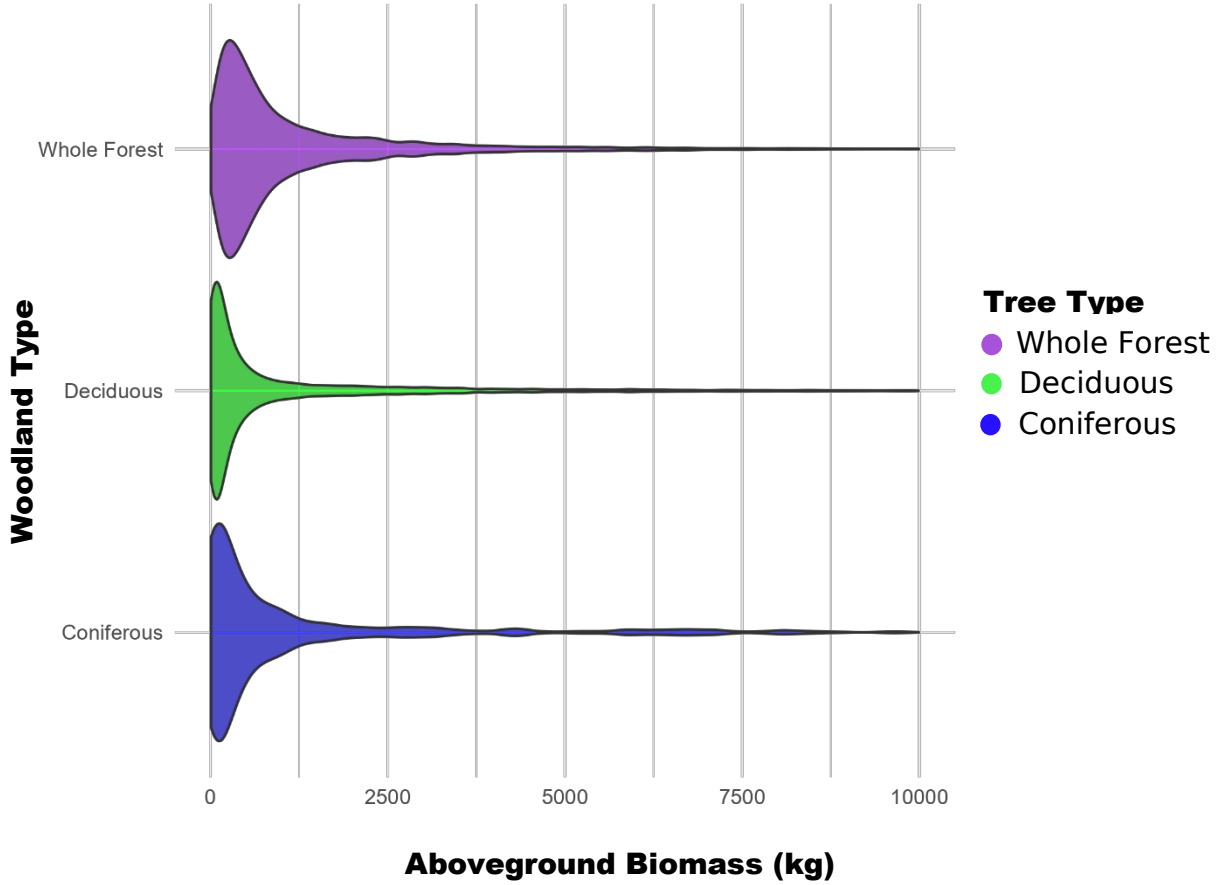

Figure 14. *Violin plot showing tree size distribution (by AGB), categorised by woodland type within Home Covert, using 2023 drone point cloud.*

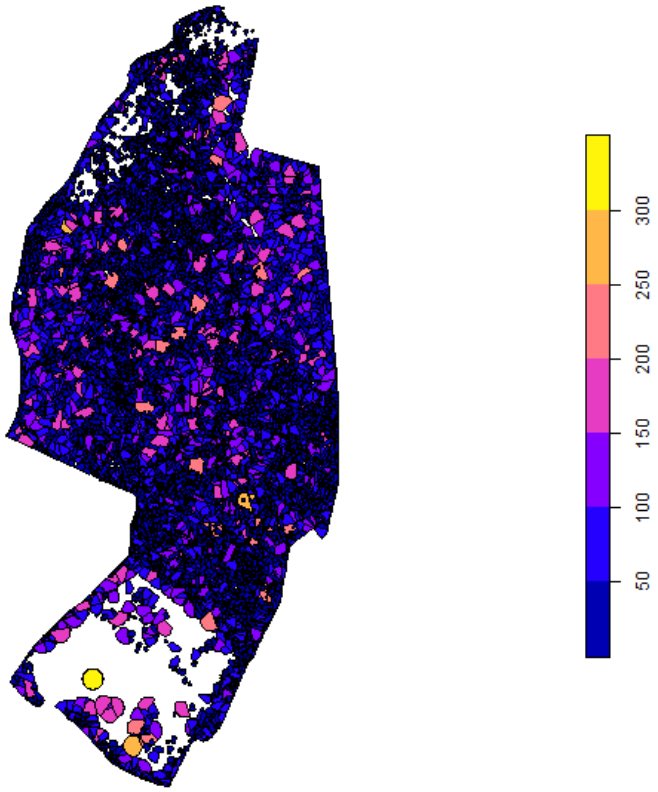

Figure 15. *Tree crown area (convex hull) of Home Covert woodland as polygons using NT 2023 point cloud data. Scale represents crown area (m²).*

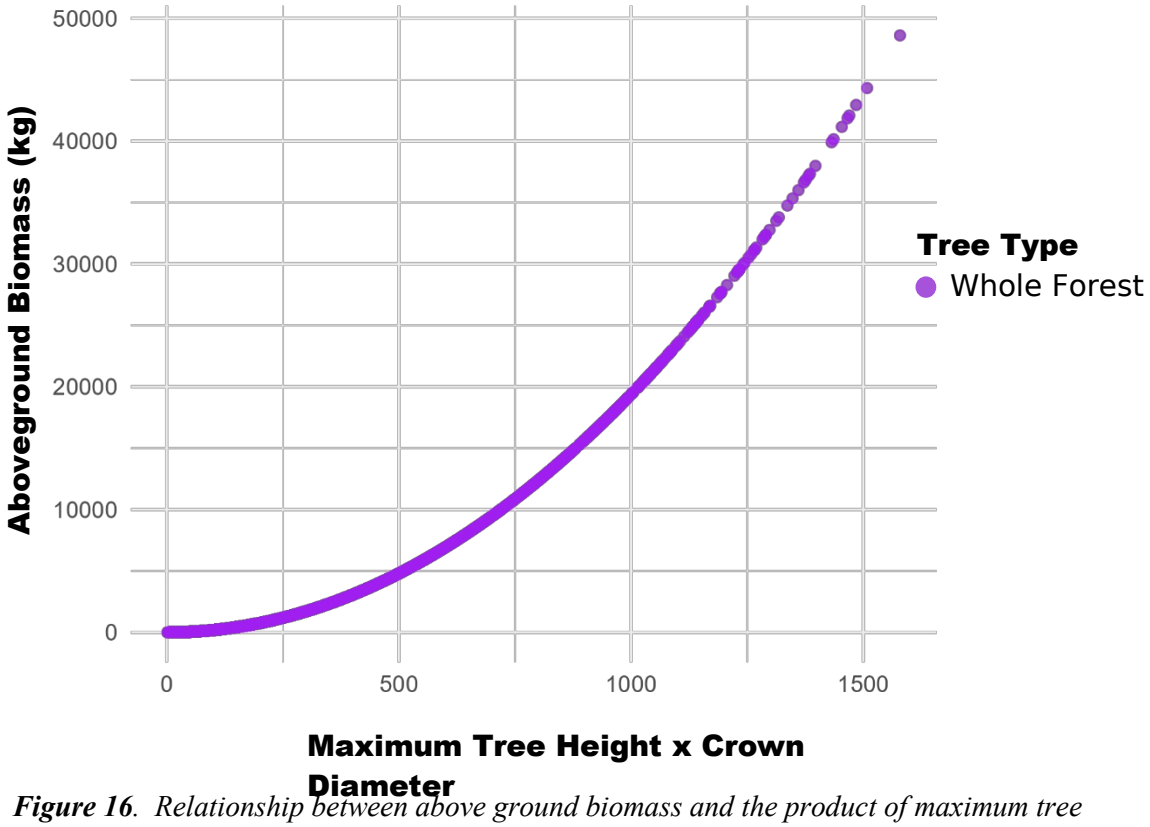

Figure 16. *Relationship between above ground biomass and the product of maximum tree height and crown diameter for whole mixed deciduous woodland, using 2023 drone point cloud.*

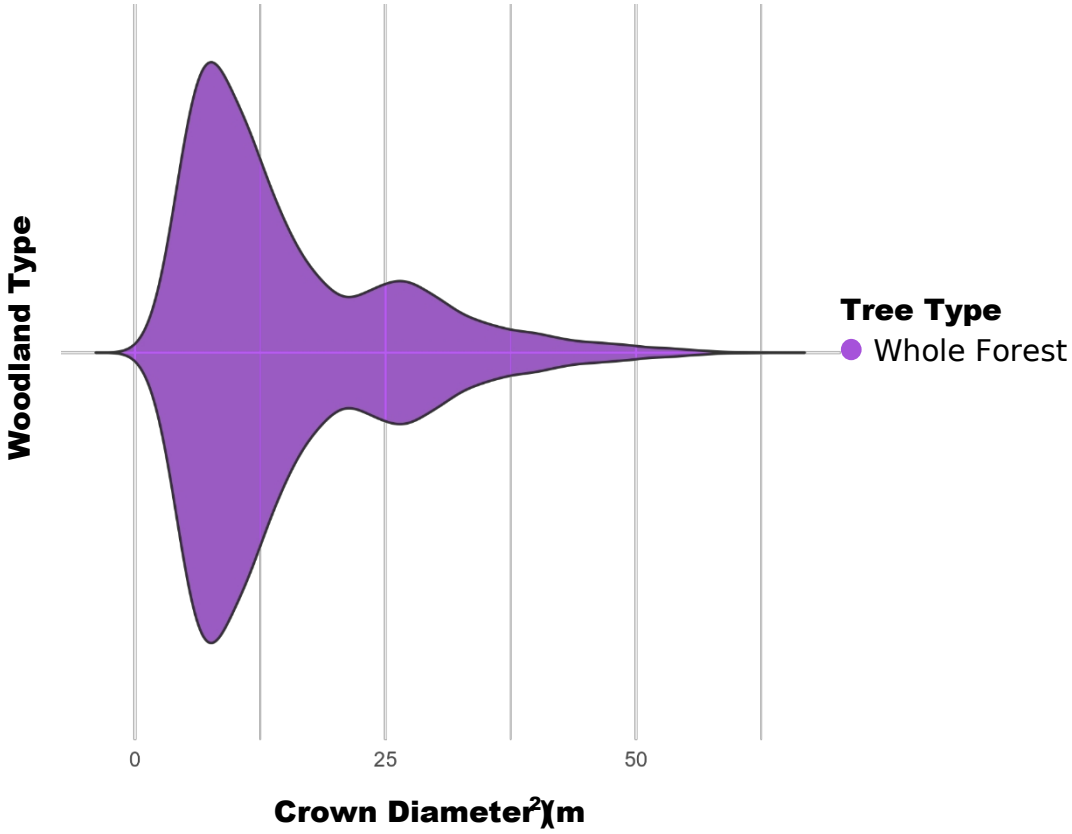

Figure 17. *Violin plot showing tree size distribution (by tree crown diameter), categorised by woodland type within Home Covert, using 2023 drone point cloud.*

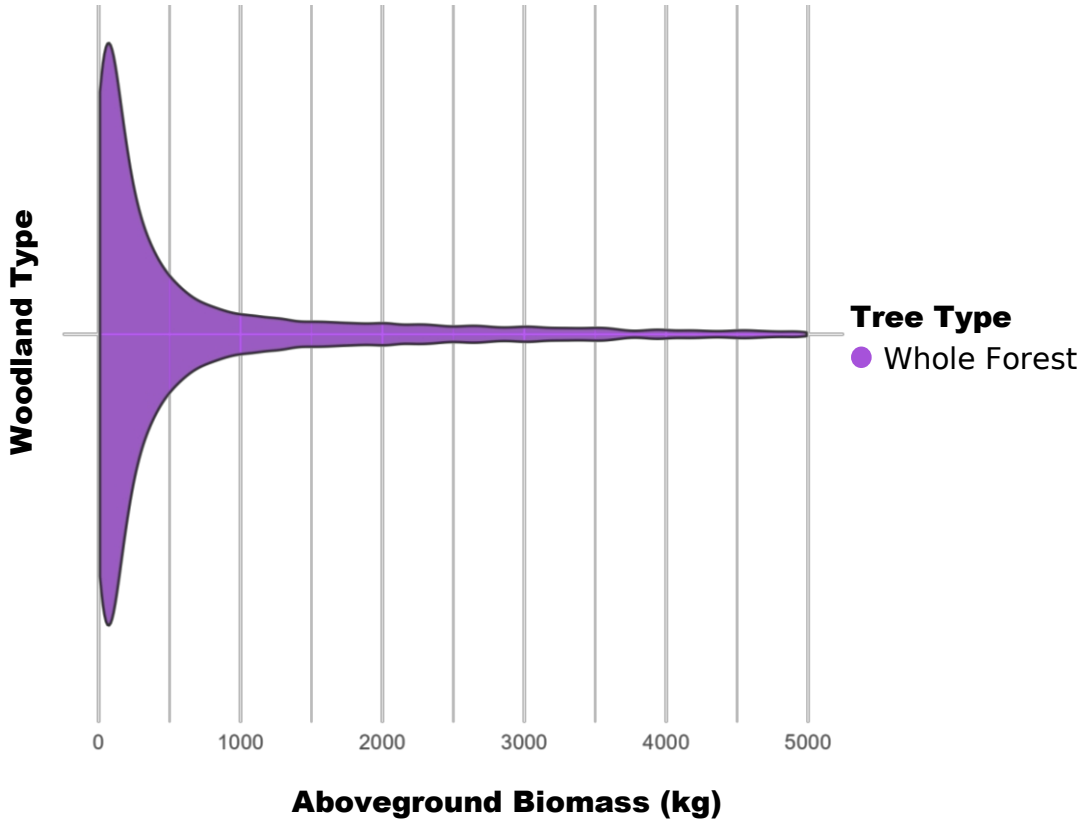

Figure 18. *Violin plot showing tree size distribution (by AGB), categorised by woodland type within Home Covert, using 2023 drone point cloud, using Jucker et al. (2017) allometric equation.*

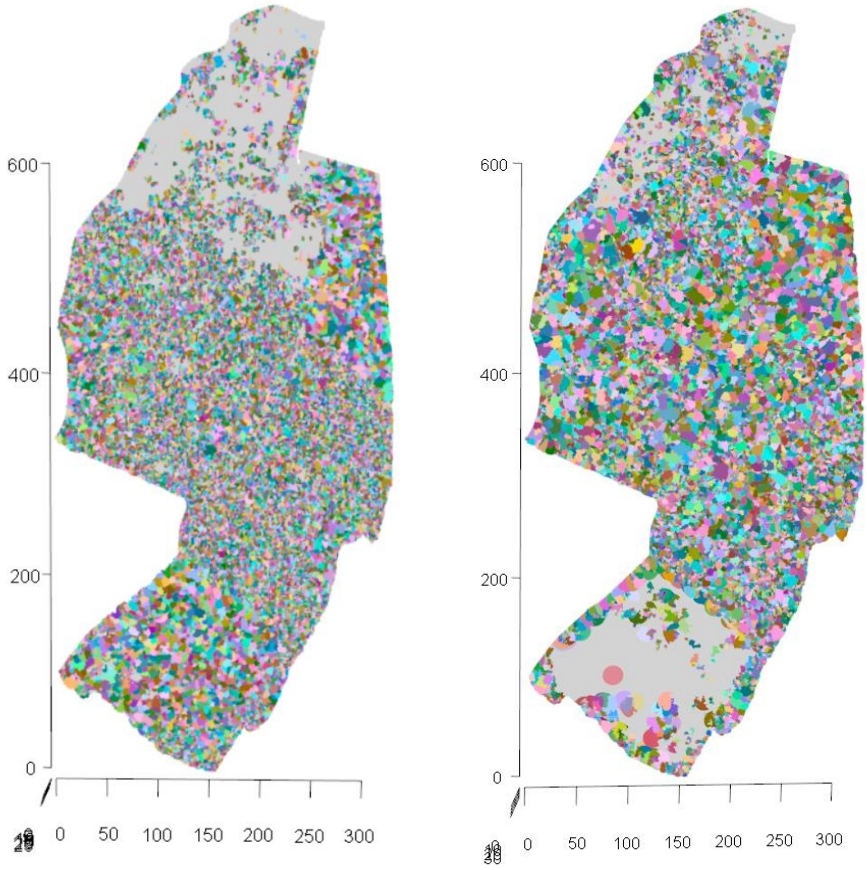

Figure 19. *Comparison of EA 2018 LiDAR point cloud (left) and 2023 drone LiDAR point cloud (right), using individual tree segmentation.*

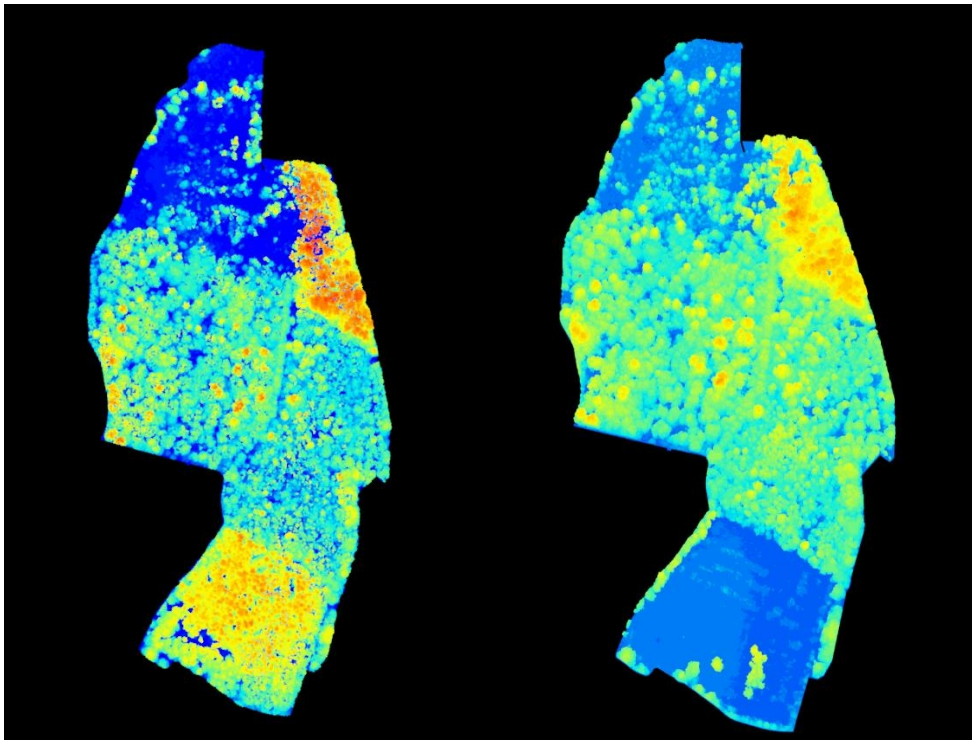

Figure 20. *Comparison of EA 2018 LiDAR point cloud (left) and 2023 drone LiDAR point cloud (right), using individual tree segmentation.*

Table 8. Ground data measurements - Tree measurements obtained using **a Suunto PM-5 Clinometer,** a 150 cm double-sided tape measure, a 30 m tape measure, and a GPS receiver.

Tree No.	**Coordinates**	**Elevation (m)**	**DBH (cm)**	**Ground distance (m)**	**a° (deg)**	**b° (deg)**	**Tree height (m)**
1	52.57403° 0.56917°	13	65.5	10.23	60.10	13.73	20.5
2	52.57386° 0.56914°	2	73.6	9.78	68.63	15.71	27.75
3	52.57436° 0.56981°	2	117 (77.9, 53.9)	8.9	75.33	18.63	37
4	52.57481° 0.57064°	10	223	17.73	48.44	4.03	21.25
5	52.57689° 0.56975°	6	134.8	20.75	44.65	4.82	22.25
6	52.57717° 0.56986°	6	81.8	14.9	54.64	8.59	23.25
7	52.57472° 0.56800°	0	143.3	18.8	48.16	3.04	22
8	52.57489° 0.56869°	-5	135.8	9.2	73.96	26.06	36.5
9	52.57550° 0.57036°	2	73.8	11.84	60.59	9.59	23
10	52.57575° 0.56992°	7	133.5	15.76	57.77	8.13	27.25

4.0 Discussion

The 2018 EA airborne LiDAR point cloud dataset, along with the National Trust's proprietary drone-based LiDAR point cloud, were utilised to extract key tree metrics, including tree count, height, crown area, and AGB within Home Covert. These results directly address the first research question posed in this study. Central to the data processing were two custom-developed scripts, '*OxburghProject_EA_LIDAR.R*' and '*OxburghProjectDrone_LIDAR.R*' which enabled a comprehensive analysis of both the EA and NT point clouds. In addition to successfully estimating AGB, the methodology also facilitated the estimation of aboveground carbon storage, providing key evidence in support of the second research question. Furthermore, the processing and visualisation of both point clouds within the R Statistical Software (R Studio environment) enabled a detailed comparison of the two LiDAR datasets, highlighting distinctions between the high-resolution drone point cloud and the EA LiDAR dataset. The forthcoming sections will delve deeper into the implications of these results, exploring their broader significance in relation to the study's objectives.

1. **Airborne LiDAR utility in Woodand Metrics**
   How effective is airborne LiDAR in determining tree count, height, crown area, and above ground biomass in woodlands?

Tree metrics were primarily extracted using the lidR package in R Studio, a tool specialised for processing airborne LiDAR point clouds (Roussel *et al.*, 2020). The package utilises individual tree segmentation (ITS), a common method in forestry for identifying treetops, delineating crown boundaries, and calculating tree attributes. As previously addressed, ITS accuracy depends on precise tree identification and can be prone to errors, particularly in over- or underestimating crown dimensions (Roussel *et al.*, 2020; White *et al.*, 2016). To address these limitations, the Li2012 segmentation algorithm (Li *et al*., 2012) was applied, enabling direct point cloud processing without the need for rasterisation or CHM generation, resulting in more efficient and accurate tree metric extraction.

The application of airborne LiDAR for determining tree count, height, crown area, and AGB within Home Covert proved to be effective. This is evidenced by the substantial AGB values extracted from the EA 2018 and NT 2023 LiDAR datasets, as shown in **Table 7**. The EA 2018 dataset estimated a total AGB of **8,189,443.04 kg (511,840.19 kg/ha)**, while the 2023 drone dataset yielded a significantly higher estimate of **17,800,412 kg (1,112,525.75 kg/ha)**. These AGB estimates were derived using group species-specific allometric equations from Jucker *et al.* (2017) (Equation 2), using allometric values for the specific Palearctic woodland types ~ mixed deciduous and coniferous woodlands (**Table 2**).

The initial AGB calculations employed a generalised woodland allometric equation (Equation 1), adapted from the models of Wilkes *et al.* (2018), Aabeyir *et al.* (2022), and Muumbe *et al.* (2024). However, this approach was found to be overly broad and lacked specificity. The results derived from this generalised equation (**see Appendix 9, Table 1 and 2**) were ultimately disregarded, as they failed to account for the significant presence of pine

plantations and coniferous species in the southern region of Home Covert, particularly in the 2018 EA dataset.

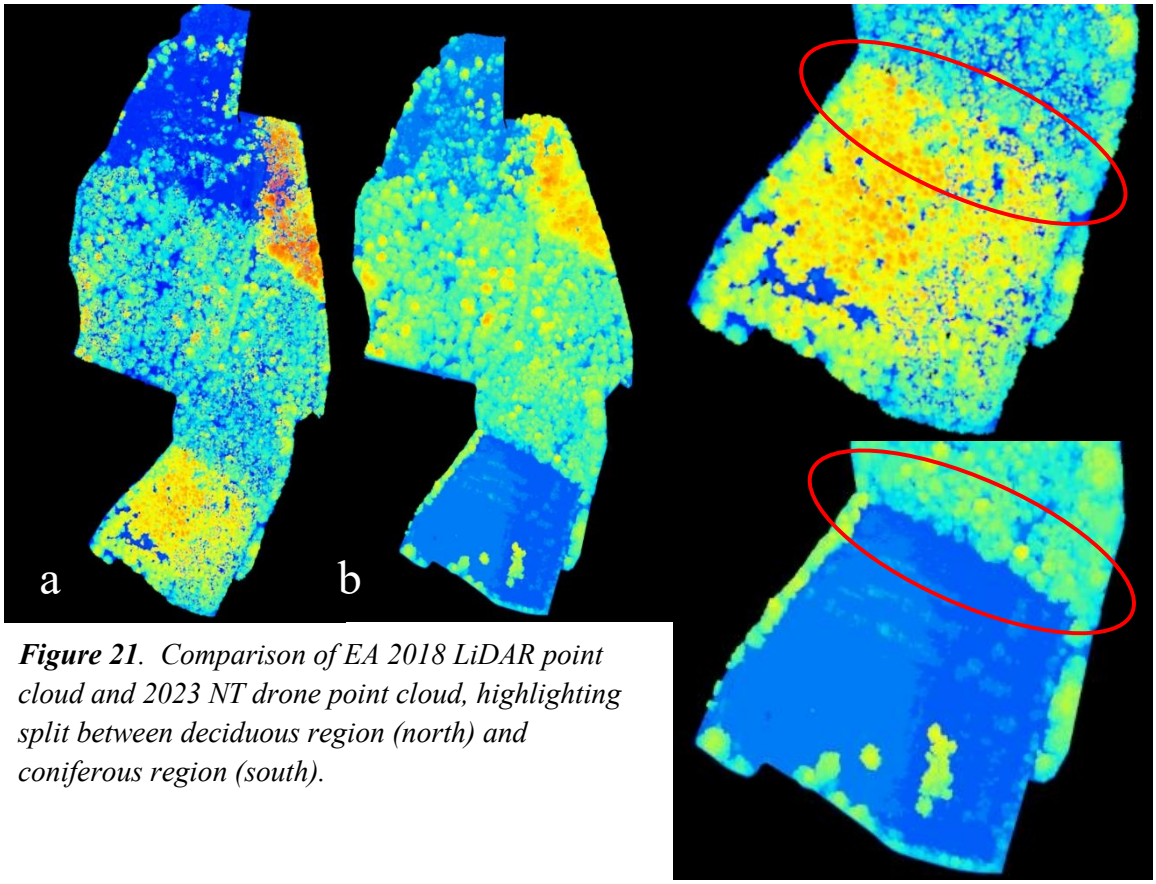

Figure 21. *Comparison of EA 2018 LiDAR point cloud and 2023 NT drone point cloud, highlighting split between deciduous region (north) and coniferous region (south).*

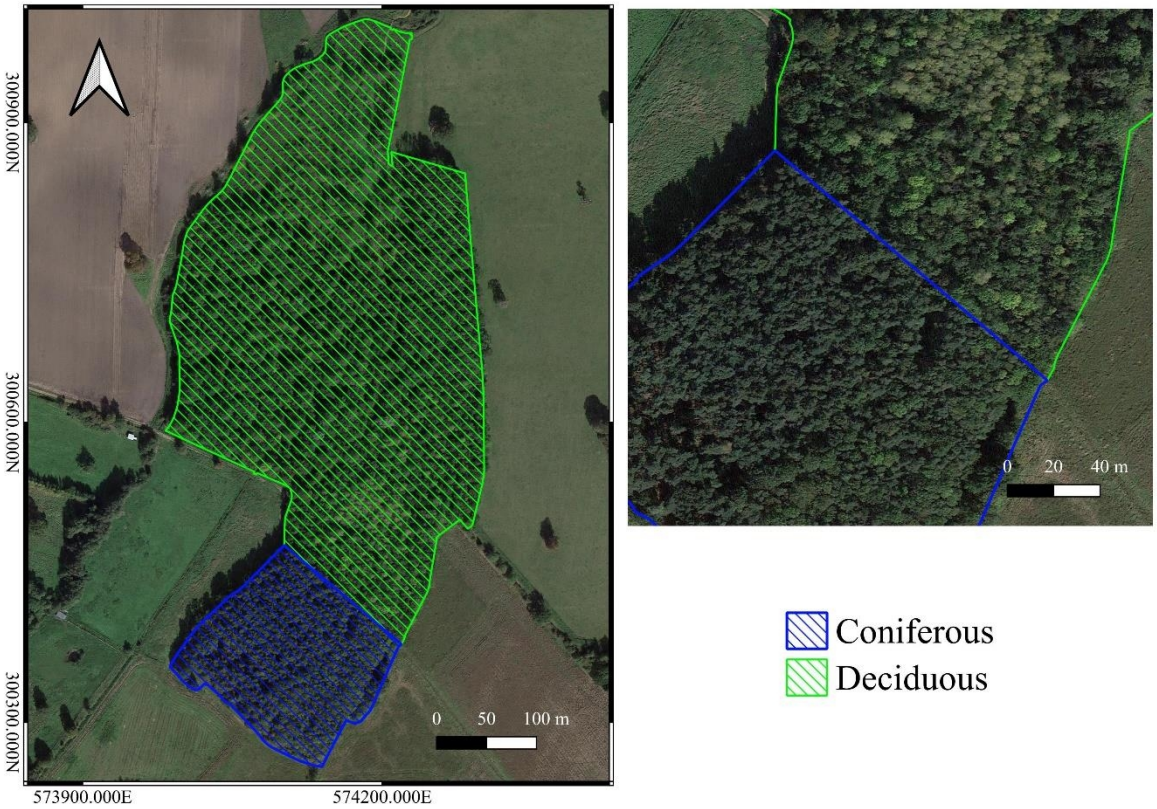

Figure 22. *Distinguishing Home Covert woodland types; coniferous woodland (south) in blue, mixed deciduous woodland (north) in green. Used Google Satellite basemap.*

To improve accuracy, the study area was divided into deciduous (northern) and coniferous (southern) regions, enabling the application of group species-specific equations from Jucker *et al.* (2017), which are well established equations for woodland AGB estimation. This approach was applied to the EA 2018 dataset. While the NT 2023 drone dataset was initially processed by separately analysing coniferous and deciduous populations, it was later treated as a mixed temperate deciduous woodland due to pre-drone survey pine plantation felling (**see Appendix 9, Table 3**). This adjustment facilitated a more consistent and accurate comparison between the two datasets. The division of the woodland was achieved through the use of GIS by segmenting the Home Covert woodland shapefile into two distinct regions (**Figure 21 and 22**). This division was based on a detailed analysis of the EA point, which revealed significant differences in tree density between the southern coniferous pine plantation, characterised by tightly packed trees, and the northern region, consisting of more spaced and diverse mixed deciduous woodland (**Figure 23**). The NT point cloud allowed for an ultimate clear distinction between coniferous woodland (where pine tree felling took place) and the mixed deciduous woodland.

Figure 23. *Distinguishing Home Covert woodland types using NT orthomosaic; coniferous woodland (north) in blue, mixed deciduous woodland (south) in green.*

2. **Carbon Storage**
   What is the aboveground carbon storage in this woodland stand, and how confident should we be in this estimate?

The selected equation for estimating tree carbon content leverages the established biomass-to-carbon ratio of 47% for dry wood, as reported by Chave *et al.* (2019). This ratio is supported by a consensus in the literature and is used for carbon content estimations in biomass (Fawcett *et al.*, 2022). Furthermore, research indicates that the dry weight of wood constitutes approximately 72.5% of the green weight or AGB (Hanif *et al.*, 2015).

The equation used was:

$$\mathbf{C = AGB \times 0.725 \times 0.47C}$$

where C represents the carbon content and AGB denotes aboveground biomass. This formula first derives the dry weight of the tree and subsequently calculates the carbon content based on the 47% carbon ratio. To estimate the corresponding CO_2 sequestration, the carbon content is multiplied by a factor of 3.67, which accounts for the carbon-to-oxygen ratio in CO_2 (Hanif *et al.*, 2015).

Using the methodology highlighted previously, the carbon storage and carbon sequestration of Home Covert was able to be estimated. According to **Table 7**, the EA point cloud data estimated the total carbon content at **2,790,552.72 kg** (174,409.54 kg/ha), with a corresponding CO_2 sequestration estimate of **10,241,328.47 kg** (640,083 kg/ha). In contrast, the drone point cloud data estimated the total carbon content at **6,065,490.39 kg** (379,093.15 kg/ha), and the CO_2 sequestration at **22,260,349.73 kg** (1,391,271.86 kg/ha). These estimates pertain solely to aboveground carbon storage and sequestration, excluding belowground carbon in roots and soil.

It is important to acknowledge that the methodology used for calculating woodland carbon content does not fully adhere to the best practices outlined in the FC Woodland Carbon Code: Carbon Assessment Protocol (v2.0) (Jenkins *et al.,* 2018). This protocol emphasises traditional field measurement and estimation techniques for calculating stored carbon in woodlands and stresses the importance of estimating the confidence of these measurements.

In this study, confidence intervals for AGB and carbon content estimates were not calculated, as the equations were applied directly to tree metrics without statistical analysis. Incorporating statistical models in future work to determine the range within which true values are likely to fall would enhance the robustness of these estimates by providing confidence intervals.

Thus, while the methodology applied provides valuable insights into carbon content and sequestration, it falls short of the comprehensive standards recommended by the FC Woodland Carbon Code. Addressing these limitations and integrating confidence measures into future assessments would significantly improve the accuracy and reliability of carbon estimation.

3. **Comparison of LiDAR data sources**
   How do drone-derived high resolution LiDAR surveys compare with open source Environment Agency LiDAR in utility for woodland metrics?

Tables 3 and 5 present tree attributes derived from the EA and drone LiDAR point clouds, using functions such as `'crown_metrics'` and `'tree_metrics'`. Following tree segmentation, maximum tree heights were used to represent individual trees, as shorter understory trees are more difficult to accurately delineate. The EA point cloud identified **19,789** trees total, while the drone point cloud detected approximately **10,577** trees total (**Figure 19 and 20** for ITS comparison). These discrepancies arise from differences in the ITS process, specifically through the use of the '`segment_trees`' function in the lidR package.

Key to these differences were adjustments to the li2012 algorithm's parameters, '*dt1*' and '*dt2*', which control the distance thresholds for tree height segmentation. Lowering '*dt1*' increases the algorithm's sensitivity to height variations, resulting in more distinct tree crowns, while reducing '*dt2*' tightens the vertical range within each segment, improving the separation of individual trees. These adjustments were particularly necessary for the dense coniferous areas, where distinguishing individual crowns was challenging. Despite this success, the AGB estimate from the drone point cloud was significantly higher, suggesting that further refinement of '*dt1*' and '*dt2*' might have improved accuracy. For instance, the maximum crown area in the drone dataset was **213.97 m²** (**Table 5**), which is unrealistically large. This indicates that incorrect parameter choices can lead to inaccurate results. Important to consider, in dense woodland structure with overlapping canopies, even strict parameters might not eliminate. Fine-tuning this process helps to achieve more distinct tree segments with minimal overlap in the LiDAR point cloud. Therefore, selecting appropriate ITS parameters is critical for ensuring reliable tree metrics.

Another important consideration is that the drone dataset (300+ points/m²) has a significantly higher resolution compared to the EA dataset (8 points/m²). This higher point density could mean that the drone-derived AGB estimates are more accurate, as it likely captures finer details that the EA data may have missed. However, without sufficient ground-based measurements for comparison, it is difficult to definitively determine which dataset provides more accurate results. To resolve this uncertainty, ground data would be required to perform a cross-analysis. This could be achieved through linear regression, comparing LiDAR-derived tree heights with ground-based measurements. Such an analysis would allow for the calculation of the coefficient of determination (R^2), slope, and intercept, providing a clearer assessment of how well the LiDAR measurements reflect actual tree heights and crown metrics. This, in turn, would lead to more reliable and accurate AGB estimates. A further consideration to improve the accuracy of the AGB results, could include the development of tree classification models to distinguish individual tree species within the woodland and where they are located. These models allow for the application of species-specific allometric equations, rather than the generalised woodland-type equations used in this study. However, the development of such models is time-consuming and falls outside the scope of this project.

Nonetheless, species-specific classifications would significantly enhance the precision of biomass estimates and other tree metrics.

The tree crown areas in Home Covert, represented as polygons for both the drone and EA point clouds, are visually depicted in **Figures 7 and 15**. The drone point cloud clearly shows larger tree crown areas, as well as the lack of vegetation coverage in the southern region due to post-pine felling. This visualisation effectively illustrates the estimated size of individual trees within Home Covert, highlighting the variation in crown areas between the two LiDAR datasets. These differences are primarily attributable to the application of the Li2012 algorithm for ITS and the varying point densities between the datasets.

The creation of a CHM enabled the visualisation of tree height distribution across Home Covert. Despite being generated through rasterisation, a comparison between the EA CHM (**Figure 6**) and the NT drone CHM (**Figure 11**) reveals significant differences in vegetation, particularly in the southern region due to the felling of pine trees. Interestingly, **Figure 6** also shows that the coniferous plantation in the south included the tallest trees (25 metres and above), which were at peak maturity prior to being felled, as evidenced by the CHM. **Figure 11**, derived from drone data, indicates considerable tree growth across the entire mixed deciduous woodland, with the northern region showing increased density compared to **Figure 6**. Additionally, it highlights the substantial growth within the woodland over the five-year gap between data acquisitions. This visual representation supports the AGB estimates obtained in this study.

The computational time required to run the '*OxburghProject_EA_LIDAR.R*' script for processing the EA point cloud was approximately **18 minutes**. This included point cloud cleaning steps, such as normalisation, the removal of negative values, and visualisation. In contrast, the processing time for the '*OxburghProjectDrone_LIDAR.R*' script exceeded **48 hours** due to the intensive computational demands of handling the significantly larger drone LiDAR point cloud, which initially measured 20.3 GB, compared to the smaller EA point cloud measured 144 MB. Downloading the original drone dataset, provided by Keith Challis, Remote Sensing Coordinator at the National Trust, took 12 hours. Although density reduction was applied to the drone point cloud to optimise processing, determining the appropriate reduction level required careful consideration. The goal was to balance reducing the file size without sacrificing too much detail, and conclusively, an 80% reduction was chosen, resulting in a 3.7 GB point cloud that allowed for detailed analysis within a manageable computational timeframe. A lesser reduction (e.g., 70%) remained too large for R Studio to process efficiently, preventing proper plotting and analysis.

Given the scale of the drone dataset, outputs such as cleaned point clouds were stored on an external hard drive with sufficient storage capacity. The challenges faced during this process, including several instances where R Studio crashed, highlight the limitations of processing high-resolution drone data in R Studio. These issues raise questions about the practicality of using such high-resolution point clouds when significant reductions are necessary for software compatibility. Regular uploads to GitHub ensured data preservation throughout this

process. These limitations are important to consider when working with large LiDAR datasets.

It is important to highlight a key advantage of the drone-derived point cloud, beyond its substantially higher spatial resolution (300+ points/m²) compared to the EA dataset (8 points/m²): drone surveys can be conducted at any time, allowing for near real-time data collection and rapid AGB estimates, as long as the necessary drone and LiDAR equipment are available. In contrast, the EA dataset is temporally limited, with the most recent survey conducted in 2018, creating a significant six-year gap. Given that deciduous trees can grow significantly each year, with *Acer saccharinum* (Silver Maple) reaching up to 1.5 metres per year (Ferus, 2023; Ashby *et al.*, 1992), this gap means the EA dataset does not provide an accurate reflection of Home Covert's current AGB. Although a 2021 National LiDAR point cloud from the Environment Agency is available (**Figure 24**), it unfortunately does not cover the Home Covert woodland, which underscores a major limitation of relying on EA LiDAR products for ongoing or current analysis.

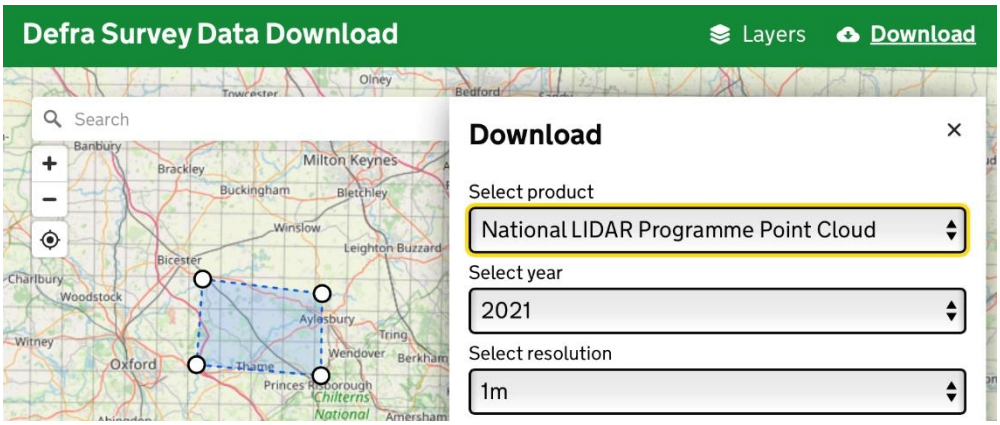

***Figure 24**. 2021 EA LiDAR point cloud available on Defra Survey Data Download.*

Comparison of AGB estimates

A combination of scatterplots and violin plots was employed to visualise and compare tree metrics derived from the analysis of both the EA and drone LiDAR point clouds.

Figures 8 to 10 present the tree metrics from the EA point cloud, revealing that the coniferous region of the woodland (southern section) holds the highest AGB, compared to the deciduous areas. This aligns with earlier analysis, which indicated a denser coniferous stand in the EA point cloud, with coniferous trees at peak height and maturity. However, **Figure 9** shows that both deciduous and coniferous woodlands exhibit similar tree crown diameters, with the majority falling between 0 to 10 m². In contrast, **Figures 13 and 14** (drone point cloud data) show a broader distribution of crown diameters, extending up to 40 m². This may be attributed to the higher resolution of the drone LiDAR, which provides more accurate delineation of tree crowns and more points to base analysis off.

Figures 17 and 18 depict the entire woodland of Home Covert without separating deciduous and coniferous areas. Violin plots for both the EA 2018 and drone datasets show AGB estimates for the entire forest, using a generalised allometric equation. Additionally, AGB estimates for the deciduous and coniferous sections were calculated using Jucker *et al.*'s group species-specific allometric equations. The drone data also includes AGB estimates based on Jucker's deciduous parameters, reflecting the predominance of mixed deciduous woodland following pine felling.

Overall, the results indicate that AGB estimates can be derived proficiently from both EA and drone LiDAR datasets. However, future research would benefit from a larger project incorporating ground data to validate the accuracy of the point cloud-derived estimates. This validation would determine the level of precision needed for different applications, helping to decide whether EA LiDAR, with its lower resolution, is sufficient or if higher-resolution drone data is required for more accurate measurements.

Ground Data

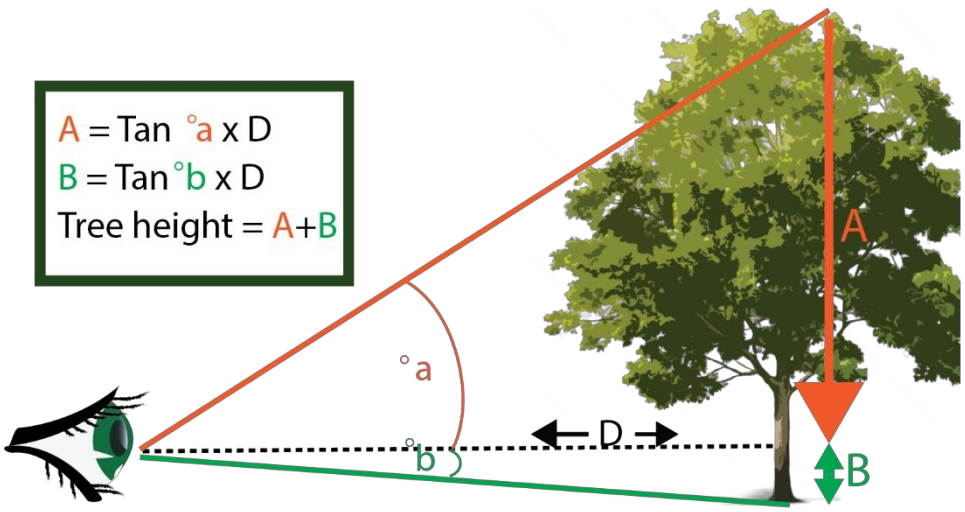

Figure 25. *Tree trigonometry to calculate tree height using clinometer measurements obtained at fieldwork. Illustration made by Amber McDonagh.*

Tree heights were estimated during fieldwork using trigonometric calculations based on clinometer measurements (**Figure 25**), with the results presented in **Table 8**. This method, grounded in well-established principles of tree height measurement, has been widely applied in forestry and woodland management research (Bilous *et al.*, 2021; Stereńczak *et al.*, 2019; Williams *et al.*, 1994).

Although ground-based measurements were collected to facilitate comparison between LiDAR data and field data, they were not extensively utilised in this analysis. The focus of the project was not on assessing the absolute accuracy of the LiDAR data but rather on evaluating the process of obtaining tree metrics and comparing the results from different LiDAR sources. However, incorporating more ground data and calculating metrics such as

root mean square error (RMSE) would improve the accuracy of future assessments, offering more reliable insights for organisations like the National Trust.

Future studies with a broader scope could benefit from integrating ground-based measurements to enhance the precision of LiDAR-derived estimates. This raises the question of how much precision is truly required. Is centimetre-level accuracy necessary, or would a slight margin of error still meet the objectives? The balance between accuracy and practicality is an important consideration for woodland management applications.

Key limitations & Recommendations

1. Processing Time and Computational Efficiency

- **Drone Data Processing**: The drone dataset took approximately **48 hours** to process, even with density reduction to 20% of the original dataset, which caused a loss of point richness. Without this reduction, processing would have been even longer. This limitation affects the accuracy of tree metrics such as crown area and height.
- **EA Dataset Processing**: In comparison, the EA dataset was significantly smaller (144 MB vs. 20.3 GB), requiring only **18 minutes** to process. The quicker processing time for the EA dataset demonstrates a more efficient workflow, though it comes at the cost of lower resolution and outdated data.

Implications:

- The extensive time needed to process high-resolution drone data may limit its application in projects where rapid decision-making is required.

Recommendation: For future projects, the National Trust should weigh the trade-offs between resolution and processing time, considering whether such high-density data is required for all woodland areas or only specific **high-priority sites**.

2. Loss of Point Richness and its Effect on Accuracy

- The reduction in point density from **300+ points/m²** to a more manageable size (resulting in 80% reduction) inevitably compromised the precision of the derived metrics, including tree height and crown dimensions. This could result in an over- or under-estimation of attributes like AGB.
- Drone LiDAR produced higher AGB estimates (17,800,412 kg vs. 8,189,443.04 kg from EA LiDAR), partly because of the finer detail captured by the higher density. However, this precision is difficult to validate without extensive ground data comparison.

Recommendation: Where possible, avoid excessive data reduction in areas critical to the NT's conservation goals. More efficient workflows or software might help handle larger datasets without compromising detail. Incorporating ground data would improve the reliability of drone-derived estimates.

3. Lack of Ground Data for Validation

- While tree heights were measured during fieldwork, they were not extensively utilised for validating the LiDAR estimates. The lack of ground-based validation introduces uncertainty, especially in AGB and carbon storage estimates.
- True validation requires root mean square error (RMSE) or other statistical measures to compare LiDAR-derived metrics with actual field measurements.

Recommendation: The NT should prioritise ground data collection for future projects to validate LiDAR-derived tree metrics. This would increase confidence in the outputs and align with best practices like the FC Woodland Carbon Code.

4. Comparison of Open-Source vs. Proprietary Data

- The EA LiDAR is open source but has limitations, including lower point density (8 points/m^2) and being outdated (2018 data). Despite being less accurate, it provides a cost-effective option for large-scale, non-urgent surveys.
- The drone LiDAR, on the other hand, offers up-to-date, high-resolution data, but comes with significantly higher costs and processing demands.

Recommendation: NT should adopt a hybrid approach, using EA LiDAR for broad woodland assessments and deploying drone LiDAR for more targeted, high-importance areas where finer metrics are critical.

5. Generalisability and Broader Application

- The methodologies and findings from the **Home Covert** project could be applied to other National Trust woodland sites. However, the limitations in data processing and validation mean the approach may not be suitable for all environments without adaptations.
- The lack of ground data makes it harder to generalise findings across different woodland types, especially where tree species or structures differ.

Recommendation: When applying this methodology to other sites, consider the specific tree compositions and woodland structure, and whether these align with the assumptions made in the Home Covert analysis. Ground data should be integrated into any large-scale application to ensure results remain reliable.

6. Implications for Carbon Storage Estimates

- While the study estimated carbon storage (using a standard biomass-to-carbon ratio), it lacked confidence intervals or statistical validation, which would strengthen the

estimates. Moreover, the exclusion of belowground biomass and reliance on allometric equations may introduce errors.

- Additionally, the methods used do not fully align with the FC Woodland Carbon Code, which emphasises ground measurements for comprehensive carbon assessments.

Recommendation: Future carbon storage studies should include confidence intervals and align with the Woodland Carbon Code to improve the accuracy and reliability of results. Additionally, including belowground biomass would provide a fuller picture of the woodland's carbon sequestration capacity.

5.0 Conclusion

In conclusion, this study effectively addresses the research questions through a comprehensive analysis of airborne and drone-based LiDAR datasets. First, the question regarding the utility of airborne LiDAR in determining tree metrics such as count, height, crown area, and AGB was answered with positive results. The application of the *lidR* package and group species-specific allometric equations allowed for accurate extraction of tree metrics, despite some limitations in the segmentation algorithm. The comparison between Environment Agency (EA) and National Trust (NT) LiDAR data highlighted the superior precision of drone-derived metrics, although the EA data still proved useful for broader assessments, particularly where cost and time efficiency are critical. Thus, airborne LiDAR was shown to be effective, though the higher-resolution drone data provided more accurate results spatially and temporally.

The second research question concerning the estimation of aboveground carbon storage was also addressed successfully. By applying an established biomass-to-carbon ratio, carbon storage and sequestration were calculated for Home Covert, providing valuable insights into the woodland's carbon dynamics. However, the lack of confidence intervals and reliance on purely LiDAR-derived estimates means that these results, while informative, would benefit from validation through ground-based measurements. Future work incorporating statistical models and adhering more closely to protocols like the FC Woodland Carbon Code would further enhance the reliability of these estimates.

Lastly, the study effectively compared the utility of drone-derived high-resolution LiDAR with EA's open source data. The higher resolution of the drone dataset led to higher detail (potentially higher accurate) AGB and tree metric estimates, though it required significantly more processing time and computational resources. The results suggest that both data sources have their place in woodland management: EA LiDAR is a cost-effective option for large-scale, non-urgent surveys, while drone LiDAR is better suited for precise, site-specific assessments.

In summary, while the research achieved its objectives, future studies should aim to integrate ground validation and consider improvements in computational efficiency, especially when handling large, high-resolution datasets. Incorporating these elements would refine the

accuracy of woodland metrics and carbon storage estimates, providing more reliable data for conservation efforts and woodland management.

6.0 Open Research

GitHub Repository: https://github.com/TESS-Laboratory/McDonagh_trees_from_lidar

Environment Agency LiDAR data: https://www.data.gov.uk/dataset/f0db0249-f17b-4036-9e65-309148c97ce4/national-lidar-programme
https://environment.data.gov.uk/DefraDataDownload/?Mode=survey

National Trust Data using Emapsite Contractor Link: https://www.emapsite.com/online-services/data-sharing/contractor-link

7.0 Acknowledgements

I would like to express my heartfelt gratitude to my dissertation supervisor, Dr. Andrew Cunliffe, for his unwavering support, expert guidance, and invaluable insights throughout this journey. His deep expertise in R Studio and remote sensing has been instrumental in navigating the complexities of this project, particularly in the analysis of remote sensing data for terrestrial ecosystems. I am immensely grateful for his patience in addressing my numerous queries and emails. Without his mentorship, this dissertation would not have been possible.

I would also like to extend my sincere thanks to Keith Challis, my consultancy partner from the National Trust, whose encouragement and belief in this project inspired me to pursue this dissertation. It has been a privilege to collaborate with an organisation I have long admired. Thank you, Keith, for not only providing the LiDAR data essential to this study but also for allowing me the autonomy to shape the focus and direction of the project.

Additionally, I acknowledge the Environment Agency (2024), as well as the teams behind QGIS, ArcGIS, and R Studio, for providing open-access data and tools that were critical to the success of this research.

Lastly, I would like to express my deepest appreciation to my family and friends, with special thanks to my mother and grandfather, for their unwavering encouragement and inspiration. Their emotional and academic support has been a cornerstone of my ability to complete this dissertation.

To conclude, I would also like to acknowledge the use of ChatGPT, which provided assistance with the creation of code scripts, in combination with GitHub resources.

8.0 References

Aabeyir, R., Adu-Bredu, S., Agyare, W. A., & Weir, M. J. C. (2020). Allometric models for estimating aboveground biomass in the tropical woodlands of Ghana, West Africa. *Forest Ecosystems*, *7*(1), 41. https://doi.org/10.1186/s40663-020-00250-3

Abich, A., Mucheye, T., Tebikew, M., Gebremariam, Y., & Alemu, A. (2019). Species-specific allometric equations for improving aboveground biomass estimates of dry deciduous woodland ecosystems. *Journal of Forestry Research*, *30*(5), 1619–1632. https://doi.org/10.1007/s11676-018-0707-5

Abirami, B., Radhakrishnan, M., Kumaran, S., & Wilson, A. (2021). Impacts of global warming on marine microbial communities. *Science of The Total Environment*, *791*, 147905. https://doi.org/10.1016/j.scitotenv.2021.147905

Adam, M., Urbazaev, M., Dubois, C., & Schmullius, C. (2020). Accuracy Assessment of GEDI Terrain Elevation and Canopy Height Estimates in European Temperate Forests: Influence of Environmental and Acquisition Parameters. *Remote Sensing*, *12*(23), 3948. https://doi.org/10.3390/rs12233948

Aljumaily, H., Laefer, D. F., Cuadra, D., & Velasco, M. (2023). Point cloud voxel classification of aerial urban LiDAR using voxel attributes and random forest approach. *International Journal of Applied Earth Observation and Geoinformation*, *118*, 103208. https://doi.org/10.1016/j.jag.2023.103208

Araza, A., de Bruin, S., Hein, L., & Herold, M. (2023). Spatial predictions and uncertainties of forest carbon fluxes for carbon accounting. *Scientific Reports*, *13*(1), 12704. https://doi.org/10.1038/s41598-023-38935-8

Aricak, B., Wing, M. G., & Akay, A. E. (2022). State of the Art on Airborne LiDAR Applications in the Field of Forest Engineering. In M. N. Suratman (Ed.), *Concepts and Applications of Remote Sensing in Forestry* (pp. 357–369). Springer Nature. https://doi.org/10.1007/978-981-19-4200-6_18

Ashby, W. C., Bresnan, D. F., Roth, P. L., Preece, J. E., & Huetteman, C. A. (1992). Nursery establishment, phenology and growth of silver maple related to provenance. *Biomass and Bioenergy*, *3*(1), 1–7. https://doi.org/10.1016/0961-9534(92)90014-H

BBC News - Rare-breed horses help clear woodland at Oxburgh Estate. (2023, January 21). *BBC News*. https://www.bbc.com/news/uk-england-norfolk-64359255

Bilous, A. M., Diachuk, P. P., Zadorozhniuk, R. M., Matsala, M. S., & Burianchuk, M. M. (2021). Accuracy of selected methods of measurement of tree heights. *Ukrainian Journal of Forest and Wood Science*, *12*(1), 6–16. https://doi.org/10.31548/forest2021.01.001

Birdsey, R. A. (1992). Carbon Storage and Accumulation in United States Forest Ecosystems, General Technical Report W0- 59, United States Department of Agriculture Forest Service, North-eastern Forest Experiment Station, Radnor, PA, August 1992.

Bonan, G. B. (2008). Forests and Climate Change: Forcings, Feedbacks, and the Climate Benefits of Forests. *Science*, *320*(5882), 1444–1449. https://doi.org/10.1126/science.1155121

Brandtberg, T., Warner, T. A., Landenberger, R. E., & McGraw, J. B. (2003). Detection and analysis of individual leaf-off tree crowns in small footprint, high sampling density lidar data from the eastern deciduous forest in North America. *Remote Sensing of Environment*, *85*(3), 290–303. https://doi.org/10.1016/S0034-4257(03)00008-7

Camarretta, N., Harrison, P. A., Bailey, T., Potts, B., Lucieer, A., Davidson, N., & Hunt, M. (2020). Monitoring forest structure to guide adaptive management of forest restoration: a review of remote sensing approaches. *New Forests*, *51*(4), 573–596. https://doi.org/10.1007/s11056-019-09754-5

Chamberlain, C. P., Sánchez Meador, A. J., & Thode, A. E. (2021). Airborne lidar provides reliable estimates of canopy base height and canopy bulk density in southwestern ponderosa pine forests. *Forest Ecology and Management*, *481*, 118695. https://doi.org/10.1016/j.foreco.2020.118695

Chave, J., Andalo, C., Brown, S., Cairns, M. A., Chambers, J. Q., Eamus, D., Fölster, H., Fromard, F., Higuchi, N., Kira, T., Lescure, J.-P., Nelson, B. W., Ogawa, H., Puig, H., Riéra, B., & Yamakura, T. (2005). Tree allometry and improved estimation of carbon stocks and balance in tropical forests. *Oecologia*, *145*(1), 87–99. https://doi.org/10.1007/s00442-005-0100-x

Chave, J., Davies, S. J., Phillips, O. L., Lewis, S. L., Sist, P., Schepaschenko, D., Armston, J., Baker, T. R., Coomes, D., Disney, M., Duncanson, L., Hérault, B., Labrière, N., Meyer, V., Réjou-Méchain, M., Scipal, K., & Saatchi, S. (2019). Ground Data are Essential for Biomass Remote Sensing Missions. *Surveys in Geophysics*, *40*(4), 863–880. https://doi.org/10.1007/s10712-019-09528-w

Chave, J., Réjou-Méchain, M., Búrquez, A., Chidumayo, E., Colgan, M. S., Delitti, W. B. C., Duque, A., Eid, T., Fearnside, P. M., Goodman, R. C., Henry, M., Martínez-Yrízar, A., Mugasha, W. A., Muller-Landau, H. C., Mencuccini, M., Nelson, B. W., Ngomanda, A., Nogueira, E. M., Ortiz-Malavassi, E., … Vieilledent, G. (2014). Improved allometric models to estimate the aboveground biomass of tropical trees. *Global Change Biology*, *20*(10), 3177–3190. https://doi.org/10.1111/gcb.12629

Clark, D. B., & Kellner, J. R. (2012). Tropical forest biomass estimation and the fallacy of misplaced concreteness. *Journal of Vegetation Science*, *23*(6), 1191–1196. https://doi.org/10.1111/j.1654-1103.2012.01471.x

Clarke, B., Otto, F., Stuart-Smith, R., & Harrington, L. (2022). Extreme weather impacts of climate change: an attribution perspective. *Environmental Research: Climate*, *1*(1), 012001. https://doi.org/10.1088/2752-5295/ac6e7d

Cunliffe, A. M., Anderson, K., Boschetti, F., Brazier, R. E., Graham, H. A., Myers-Smith, I. H., Astor, T., Boer, M. M., Calvo, L. G., Clark, P. E., Cramer, M. D., Encinas-Lara, M. S., Escarzaga, S. M., Fernández-Guisuraga, J. M., Fisher, A. G., Gdulová, K., Gillespie, B. M., Griebel, A., Hanan, N. P., … Wojcikiewicz, R. (2022). Global application of an unoccupied aerial vehicle photogrammetry protocol for predicting aboveground biomass in non-forest ecosystems. *Remote Sensing in Ecology and Conservation*, *8*(1), 57–71. https://doi.org/10.1002/rse2.228

Demol, M., Aguilar-Amuchastegui, N., Bernotaite, G., Disney, M., Duncanson, L., Elmendorp, E., Espejo, A., Furey, A., Hancock, S., Hansen, J., Horsley, H., Langa, S., Liang, M., Locke, A., Manjate, V., Mapanga, F., Omidvar, H., Parsons, A., Peneva-Reed, E., … Burt, A. (2024). Multi-scale lidar measurements suggest miombo woodlands contain substantially more carbon than thought. *Communications Earth & Environment*, *5*(1), 1–11. https://doi.org/10.1038/s43247-024-01448-x

DeWald, S., Josiah, S., Erdkamp, B. (2005). Heating With Wood: Producing, Harvesting and Processing Firewood. University of Nebraska – Lincoln Extension, *Institute of Agriculture and Natural Resources.*

Emapsite Contractor Link - licensed mapping and data for contractors. (2024). Retrieved 1 July 2024, from https://www.emapsite.com/online-services/data-sharing/contractor-link

Environment Agency (2024). *National LIDAR Programme.* Retrieved 1 July 2024, https://www.data.gov.uk/dataset/f0db0249-f17b-4036-9e65-309148c97ce4/national-lidar-programme

Explore GitHub. (2024). GitHub. Retrieved 25 July, 2024, from https://github.com/explore

Fagan, M. and DeFries, R., 2009. Measurement and monitoring of the world's forests: A review and summary of remote sensing technical capability, 2009–2015.

Fawcett, D., Cunliffe, A. M., Sitch, S., O'Sullivan, M., Anderson, K., Brazier, R. E., Hill, T. C., Anthoni, P., Arneth, A., Arora, V. K., Briggs, P. R., Goll, D. S., Jain, A. K., Li, X., Lombardozzi, D., Nabel, J. E. M. S., Poulter, B., Séférian, R., Tian, H., … Zaehle, S. (2022). Assessing Model Predictions of Carbon Dynamics in Global Drylands. *Frontiers in Environmental Science*, *10*, 790200. https://doi.org/10.3389/fenvs.2022.790200

Ferus, P. (2023). Mechanisms involved in alien maples (Acer sp.) invasion process in the Central Europe. Testing hypotheses associated with species fitness. *Urban Ecosystems*, *26*(5), 1455–1467. https://doi.org/10.1007/s11252-023-01390-4

Flora, G., G. M. Athista, L. Derisha, D. S. Devi, M. P. D. Initha, and W. Shibani. (2018). Estimation of Carbon Storage in the Tree Growth of St. Mary's College (Autonomous) Campus, Thoothukudi, Tamilnadu, India, *JETIR*, *5(8)*. https://www.jetir.org/

Fortunato, L., & Galassi, M. (2021). The case for free and open source software in research and scholarship. *Philosophical Transactions of the Royal Society A: Mathematical, Physical and Engineering Sciences*, *379*(2197), rsta.2020.0079, 20200079. https://doi.org/10.1098/rsta.2020.0079

Frederikse, T., Landerer, F., Caron, L., Adhikari, S., Parkes, D., Humphrey, V. W., Dangendorf, S., Hogarth, P., Zanna, L., Cheng, L., & Wu, Y.-H. (2020). The causes of sea-level rise since 1900. *Nature*, *584*(7821), 393–397. https://doi.org/10.1038/s41586-020-2591-3

Gaulton, R., & Malthus, T. J. (2010). LiDAR mapping of canopy gaps in continuous cover forests: A comparison of canopy height model and point cloud based techniques. *International Journal of Remote Sensing*, *31*(5), 1193–1211. https://doi.org/10.1080/01431160903380565

Gleason, C. J., & Im, J. (2012). Forest biomass estimation from airborne LiDAR data using machine learning approaches. *Remote Sensing of Environment*, *125*, 80–91. https://doi.org/10.1016/j.rse.2012.07.006

Goetz, S. J., Baccini, A., Laporte, N. T., Johns, T., Walker, W., Kellndorfer, J., Houghton, R. A., & Sun, M. (2009). Mapping and monitoring carbon stocks with satellite observations: a comparison of methods. *Carbon Balance and Management*, *4*(1), 2. https://doi.org/10.1186/1750-0680-4-2

GOV.UK. Definition of trees and woodland. (2024). GOV.UK. Retrieved 24 August 2024, from https://www.gov.uk/government/publications/definition-of-trees-and-woodland/definition-of-trees-and-woodland

Hanif, M. A., Bari, M. S., & Rahman, A. (2015). Potentiality of carbon sequestration by agroforestry species in Bangladesh. *Research on Crops*, *16*(3), 562. https://doi.org/10.5958/2348-7542.2015.00080.7

Hardaker, A. (2018). Is forestry really more profitable than upland farming? A historic and present day farm level economic comparison of upland sheep farming and forestry in the UK. *Land Use Policy*, *71*, 98–120. https://doi.org/10.1016/j.landusepol.2017.11.032

Houghton, R. A., Hall, F., & Goetz, S. J. (2009). Importance of biomass in the global carbon cycle. *Journal of Geophysical Research: Biogeosciences*, *114*(G2), 2009JG000935. https://doi.org/10.1029/2009JG000935

Hunka, N., Santoro, M., Armston, J., Dubayah, R., McRoberts, R. E., Næsset, E., Quegan, S., Urbazaev, M., Pascual, A., May, P. B., Minor, D., Leitold, V., Basak, P., Liang, M., Melo, J., Herold, M., Málaga, N., Wilson, S., Durán Montesinos, P., … Duncanson, L. (2023). On the NASA GEDI and ESA CCI biomass maps: aligning for uptake in the UNFCCC global stocktake. *Environmental Research Letters*, *18*(12), 124042. https://doi.org/10.1088/1748-9326/ad0b60

Jenkins, J. C., Chojnacky, D. C., Heath, L. S., & Birdsey, R. A. (2003). National-Scale Biomass Estimators for United States Tree Species. *Forest Science*, *49*(1), 12–35. https://doi.org/10.1093/forestscience/49.1.12

Jenkins, T., Mackie, E., Matthews, R., Miller, G., Randle, T. and White, M. 2018. *FC Woodland Carbon Code: Carbon Assessment Protocol (v2.0)*. Forestry Commission.

Jucker, T., Caspersen, J., Chave, J., Antin, C., Barbier, N., Bongers, F., Dalponte, M., Van Ewijk, K. Y., Forrester, D. I., Haeni, M., Higgins, S. I., Holdaway, R. J., Iida, Y., Lorimer, C., Marshall, P. L., Momo, S., Moncrieff, G. R., Ploton, P., Poorter, L., … Coomes, D. A. (2017). Allometric equations for integrating remote sensing imagery into forest monitoring programmes. *Global Change Biology*, *23*(1), 177–190. https://doi.org/10.1111/gcb.13388

Kam, P. M., Aznar-Siguan, G., Schewe, J., Milano, L., Ginnetti, J., Willner, S., McCaughey, J. W., & Bresch, D. N. (2021). Global warming and population change both heighten future risk of human displacement due to river floods. *Environmental Research Letters*, *16*(4), 044026. https://doi.org/10.1088/1748-9326/abd26c

Kauppi, P. E., Stål, G., Arnesson-Ceder, L., Hallberg Sramek, I., Hoen, H. F., Svensson, A., Wernick, I. K., Högberg, P., Lundmark, T., & Nordin, A. (2022). Managing existing forests can mitigate climate change. *Forest Ecology and Management*, *513*, 120186. https://doi.org/10.1016/j.foreco.2022.120186

Kellner, J. R., Armston, J., & Duncanson, L. (2023). Algorithm Theoretical Basis Document for GEDI Footprint Aboveground Biomass Density. *Earth and Space Science*, *10*(4), e2022EA002516. https://doi.org/10.1029/2022EA002516

Koch, B., Heyder, U., & Weinacker, H. (2006). Detection of Individual Tree Crowns in Airborne Lidar Data. *Photogrammetric Engineering & Remote Sensing*, *72*(4), 357–363. https://doi.org/10.14358/PERS.72.4.357

Kumar, M. S., & Donnelly, S. (2023). 'Leave Fossil Fuels in the Soil, Halt Deforestation': Stop Threatening the Planet. In S. Tripathi, R. Bhadouria, R. Singh, P. Srivastava, & R. S. Devi (Eds.), *Eco-Politics and Global Climate Change* (pp. 239–255). Springer Nature Switzerland. https://doi.org/10.1007/978-3-031-48098-0_13

Kumar, V., Ranjan, D., & Verma, K. (2021). 9 - Global climate change: the loop between cause and impact. In S. Singh, P. Singh, S. Rangabhashiyam, & K. K. Srivastava (Eds.), *Global Climate Change* (pp. 187–211). Elsevier. https://doi.org/10.1016/B978-0-12-822928-6.00002-2

Kwak, D.-A., Lee, W.-K., Lee, J.-H., Biging, G. S., & Gong, P. (2007). Detection of individual trees and estimation of tree height using LiDAR data. *Journal of Forest Research*, *12*(6), 425–434. https://doi.org/10.1007/s10310-007-0041-9

Li, W., Guo, Q., Jakubowski, M. K., & Kelly, M. (2012). A New Method for Segmenting Individual Trees from the Lidar Point Cloud. *Photogrammetric Engineering & Remote Sensing*, *78*(1), 75–84. https://doi.org/10.14358/PERS.78.1.75

Li, X., Liu, C., Wang, Z., Xie, X., Li, D., & Xu, L. (2021). Airborne LiDAR: state-of-the-art of system design, technology and application. *Measurement Science and Technology*, *32*(3), 032002. https://doi.org/10.1088/1361-6501/abc867

Liu, Y., You, H., Tang, X., You, Q., Huang, Y., & Chen, J. (2023). Study on Individual Tree Segmentation of Different Tree Species Using Different Segmentation Algorithms Based on 3D UAV Data. *Forests*, *14*(7), 1327. https://doi.org/10.3390/f14071327

Mäkipää, R., Lehtonen, A., & Peltoniemi, M. (2008). Monitoring Carbon Stock Changes in European Forests Using Forest Inventory Data. In A. J. Dolman, R. Valentini, & A. Freibauer (Eds.), *The Continental-Scale Greenhouse Gas Balance of Europe* (pp. 191–214). Springer. https://doi.org/10.1007/978-0-387-76570-9_10

Martone, M., Rizzoli, P., Wecklich, C., González, C., Bueso-Bello, J.-L., Valdo, P., Schulze, D., Zink, M., Krieger, G., & Moreira, A. (2018). The global forest/non-forest map from TanDEM-X interferometric SAR data. *Remote Sensing of Environment*, *205*, 352–373. https://doi.org/10.1016/j.rse.2017.12.002

Marzano, M., & Urquhart, J. (2020). Understanding Tree Health under Increasing Climate and Trade Challenges: Social System Considerations. *Forests*, *11*(10), 1046. https://doi.org/10.3390/f11101046

McIntire, C. D., Cunliffe, A. M., Boschetti, F., & Litvak, M. E. (2022). Allometric Relationships for Predicting Aboveground Biomass, Sapwood, and Leaf Area of Two-Needle Piñon Pine (*Pinus edulis*) Amid Open-Grown Conditions in Central New Mexico. *Forest Science*, *68*(2), 152–161. https://doi.org/10.1093/forsci/fxac001

Mehmood, I., Bari, A., Irshad, S., Khalid, F., Liaqat, S., Anjum, H., & Fahad, S. (2020). Carbon Cycle in Response to Global Warming. In S. Fahad, M. Hasanuzzaman, M. Alam, H. Ullah, M. Saeed, I. Ali Khan, & M. Adnan (Eds.), *Environment, Climate, Plant and Vegetation Growth* (pp. 1–15). Springer International Publishing. https://doi.org/10.1007/978-3-030-49732-3_1

Mitchell, R. J., Hewison, R. L., Haghi, R. K., Robertson, A. H. J., Main, A. M., & Owen, I. J. (2021). Functional and ecosystem service differences between tree species: implications for tree species replacement. *Trees*, *35*(1), 307–317. https://doi.org/10.1007/s00468-020-02035-1

Mokany, K., Raison, R. J., & Prokushkin, A. S. (2006). Critical analysis of root : shoot ratios in terrestrial biomes. *Global Change Biology*, *12*(1), 84–96. https://doi.org/10.1111/j.1365-2486.2005.001043.x

Morsdorf, F., Meier, E., Allgöwer, B. and Nüesch, D., 2003. Clustering in airborne laser scanning raw data for segmentation of single trees. *International Archives of the Photogrammetry, Remote Sensing and Spatial Information Sciences*, *34*(part 3), W13.

Muumbe, T. P., Singh, J., Baade, J., Raumonen, P., Coetsee, C., Thau, C., & Schmullius, C. (2024). Individual Tree-Scale Aboveground Biomass Estimation of Woody Vegetation in a Semi-Arid Savanna Using 3D Data. *Remote Sensing*, *16*(2), 399. https://doi.org/10.3390/rs16020399

National Trust - What does the National Trust do? (2024). National Trust. Retrieved 6 August 2024, from https://www.nationaltrust.org.uk/our-cause

National Trust - Tree planting to tackle climate change. (2024). National Trust. Retrieved 6 August 2024, from https://www.nationaltrust.org.uk/our-cause/nature-climate/climate-change-sustainability/our-ambition-to-establish-20-million-trees-to-tackle-climate-change

National Trust - Our Climate and Environment Policy. (2024). National Trust. Retrieved 6 August 2024, from https://www.nationaltrust.org.uk/who-we-are/about-us/our-climate-and-environment-policy

Nonini, L., & Fiala, M. (2021). Estimation of carbon storage of forest biomass for voluntary carbon markets: preliminary results. *Journal of Forestry Research*, *32*(1), 329–338. https://doi.org/10.1007/s11676-019-01074-w

Panzavolta, T., Bracalini, M., Benigno, A., & Moricca, S. (2021). Alien Invasive Pathogens and Pests Harming Trees, Forests, and Plantations: Pathways, Global Consequences and Management. *Forests*, *12*(10), 1364. https://doi.org/10.3390/f12101364

Pati, P. K., Kaushik, P., Khan, M. L., & Khare, P. K. (2022). Allometric equations for biomass and carbon stock estimation of small diameter woody species from tropical dry deciduous forests: Support to REDD+. *Trees, Forests and People*, *9*, 100289. https://doi.org/10.1016/j.tfp.2022.100289

Paul, K. I., Larmour, J., Specht, A., Zerihun, A., Ritson, P., Roxburgh, S. H., Sochacki, S., Lewis, T., Barton, C. V. M., England, J. R., Battaglia, M., O'Grady, A., Pinkard, E., Applegate, G., Jonson, J., Brooksbank, K., Sudmeyer, R., Wildy, D., Montagu, K. D., … Hobbs, T. (2019). Testing the generality of below-ground biomass allometry across plant functional types. *Forest Ecology and Management*, *432*, 102–114. https://doi.org/10.1016/j.foreco.2018.08.043

Paul, K. I., Roxburgh, S. H., Chave, J., England, J. R., Zerihun, A., Specht, A., Lewis, T., Bennett, L. T., Baker, T. G., Adams, M. A., Huxtable, D., Montagu, K. D., Falster, D. S., Feller, M., Sochacki, S., Ritson, P., Bastin, G., Bartle, J., Wildy, D., … Sinclair, J. (2016). Testing the generality of above-ground biomass allometry across plant functional types at the continent scale. *Global Change Biology*, *22*(6), 2106–2124. https://doi.org/10.1111/gcb.13201

Persson, Å., Holmgren, J. and Söderman, U. (2002). Detecting and measuring individual trees using an airborne laser scanner. *Photogrammetric Engineering & Remote Sensing*, 68(9), 925-932.

Pyles, M. V., Prado-Junior, J. A., Magnago, L. F. S., de Paula, A., & Meira-Neto, J. A. A. (2018). Loss of biodiversity and shifts in aboveground biomass drivers in tropical rainforests with different disturbance histories. *Biodiversity and Conservation*, *27*(12), 3215–3231. https://doi.org/10.1007/s10531-018-1598-7

R Core Team, 2022. R: A language and environment for statistical computing. https://www.r-project.org/

Rance, S. J., Mendham, D. S., & Cameron, D. M. (2017). Assessment of crown woody biomass in Eucalyptus grandis and E. globulus plantations. *New Forests*, *48*(3), 381–396. https://doi.org/10.1007/s11056-016-9563-3

Reid, C., Hornigold, K., McHenry, E., Nichols, C., Townsend, M., Lewthwaite, K., Elliot, M., Pullinger, R., Hotchkiss, A., Gilmartin, E., White, I., Chesshire, H., Whittle, L., Garforth, J., Gosling, R., Reed, T. and Hugi, M. (2021). *State of the UK's Woods and Trees 2021*, Woodland Trust.

Réjou-Méchain, M., Muller-Landau, H. C., Detto, M., Thomas, S. C., Le Toan, T., Saatchi, S. S., Barreto-Silva, J. S., Bourg, N. A., Bunyavejchewin, S., Butt, N., Brockelman, W. Y., Cao, M., Cárdenas, D., Chiang, J.-M., Chuyong, G. B., Clay, K., Condit, R., Dattaraja, H. S., Davies, S. J., … Chave, J. (2014). Local spatial structure of forest biomass and its consequences for remote sensing of carbon stocks. *Biogeosciences*, *11*(23), 6827–6840. https://doi.org/10.5194/bg-11-6827-2014

Rodríguez-Veiga, P., Quegan, S., Carreiras, J., Persson, H. J., Fransson, J. E. S., Hoscilo, A., Ziółkowski, D., Stereńczak, K., Lohberger, S., Stängel, M., Berninger, A., Siegert, F., Avitabile, V., Herold, M., Mermoz, S., Bouvet, A., Le Toan, T., Carvalhais, N., Santoro, M., … Balzter, H. (2019). Forest biomass retrieval approaches from earth observation in different biomes. *International Journal of Applied Earth Observation and Geoinformation*, *77*, 53–68. https://doi.org/10.1016/j.jag.2018.12.008

Rodríguez-Veiga, P., Wheeler, J., Louis, V., Tansey, K., & Balzter, H. (2017). Quantifying Forest Biomass Carbon Stocks From Space. *Current Forestry Reports*, *3*(1), 1–18. https://doi.org/10.1007/s40725-017-0052-5

Roussel, J.-R., Auty, D., Coops, N. C., Tompalski, P., Goodbody, T. R. H., Meador, A. S., Bourdon, J.-F., De Boissieu, F., & Achim, A. (2020). lidR: An R package for analysis of Airborne Laser Scanning (ALS) data. *Remote Sensing of Environment*, *251*, 112061. https://doi.org/10.1016/j.rse.2020.112061

Searle, E. B., & Chen, H. Y. H. (2017). Tree size thresholds produce biased estimates of forest biomass dynamics. *Forest Ecology and Management*, *400*, 468–474. https://doi.org/10.1016/j.foreco.2017.06.042

Sibona, E., Vitali, A., Meloni, F., Caffo, L., Dotta, A., Lingua, E., Motta, R., & Garbarino, M. (2017). Direct Measurement of Tree Height Provides Different Results on the Assessment of LiDAR Accuracy. *Forests*, *8*(1), 7. https://doi.org/10.3390/f8010007

Stereńczak, K., Mielcarek, M., Wertz, B., Bronisz, K., Zajączkowski, G., Jagodziński, A. M., Ochał, W., & Skorupski, M. (2019). Factors influencing the accuracy of ground-based tree-height

measurements for major European tree species. *Journal of Environmental Management*, *231*, 1284–1292. https://doi.org/10.1016/j.jenvman.2018.09.100

Stevens, C. J., Bell, J. N. B., Brimblecombe, P., Clark, C. M., Dise, N. B., Fowler, D., Lovett, G. M., & Wolseley, P. A. (2020). The impact of air pollution on terrestrial managed and natural vegetation. *Philosophical Transactions of the Royal Society A: Mathematical, Physical and Engineering Sciences*, *378*(2183), 20190317. https://doi.org/10.1098/rsta.2019.0317

The lidR package. (2024). Retrieved 29 June 2024, from https://r-lidar.github.io/lidRbook/

Tian, Y., Bian, Z., Lei, S., Ji, C., Zhao, Y., Zhang, S., Duan, L., & Sedlák, V. (2021). A Process-Oriented Method for Rapid Acquisition of Canopy Height Model From RGB Point Cloud in Semiarid Region. *IEEE Journal of Selected Topics in Applied Earth Observations and Remote Sensing*, *14*, 12187–12198. https://doi.org/10.1109/JSTARS.2021.3129472

Torres De Almeida, C., Gerente, J., Rodrigo Dos Prazeres Campos, J., Caruso Gomes Junior, F., Providelo, L. A., Marchiori, G., & Chen, X. (2022). Canopy Height Mapping by Sentinel 1 and Satellite Images, Airborne LiDAR Data, and Machine Learning. *Remote Sensing*, *14*(16), 4112. https://doi.org/10.3390/rs14164112

White, J. C., Coops, N. C., Wulder, M. A., Vastaranta, M., Hilker, T., & Tompalski, P. (2016). Remote Sensing Technologies for Enhancing Forest Inventories: A Review. *Canadian Journal of Remote Sensing*, *42*(5), 619–641. https://doi.org/10.1080/07038992.2016.1207484

Wilkes, P., Disney, M., Vicari, M. B., Calders, K., & Burt, A. (2018). Estimating urban above ground biomass with multi-scale LiDAR. *Carbon Balance and Management*, *13*(1), 10. https://doi.org/10.1186/s13021-018-0098-0

Williams, M. S., Bechtold, W. A., & LaBau, V. J. (1994). Five Instruments for Measuring Tree Height: An Evaluation. *Southern Journal of Applied Forestry*, *18*(2), 76–82. https://doi.org/10.1093/sjaf/18.2.76

Yang, J., Kang, Z., Cheng, S., Yang, Z., & Akwensi, P. H. (2020). An Individual Tree Segmentation Method Based on Watershed Algorithm and Three-Dimensional Spatial Distribution Analysis From Airborne LiDAR Point Clouds. *IEEE Journal of Selected Topics in Applied Earth Observations and Remote Sensing*, *13*, 1055–1067. https://doi.org/10.1109/JSTARS.2020.2979369

Yu, T., Ni, W., Liu, J., Zhao, R., Zhang, Z., & Sun, G. (2023). Extraction of tree heights in mountainous natural forests from UAV leaf-on stereoscopic imagery based on approximation of ground surfaces. *Remote Sensing of Environment*, *293*, 113613. https://doi.org/10.1016/j.rse.2023.113613

Zellweger, F., Flack-Prain, S., Footring, J., Wilebore, B., & Willis, K. J. (2022). Carbon storage and sequestration rates of trees inside and outside forests in Great Britain. *Environmental Research Letters*, *17*(7), 074004. https://doi.org/10.1088/1748-9326/ac74d5

Zhang, C., Zhou, Y., & Qiu, F. (2015). Individual Tree Segmentation from LiDAR Point Clouds for Urban Forest Inventory. *Remote Sensing*, *7*(6), 7892–7913. https://doi.org/10.3390/rs70607892

Zianis, D., Muukkonen, P., Mäkipää, R., & Mencuccini, M. (2005). *Biomass and stem volume equations for tree species in Europe*. FI. https://jukuri.luke.fi/handle/10024/512732

9.0 Appendix

9.1 Tables for AGB, C and CO2 estimates using Equation 1

Beneath are tables containing estimates using Equation 1 in the methodology; generalised allometric adapted from the models of Wilkes *et al.* (2018), Aabeyir *et al.* (2022), and Muumbe *et al.* (2024).

Table 1. Tree metric estimates for EA point cloud using Equation 1.

Woodland type	Average AGB per tree (kg)	Total AGB (kg/ha)	Total C (kg/ha)	Total CO2 (kg/ha)
Whole temperate forest	822.76	802,606.06	273,488.01	1,003,700.99

Table 2. Tree metric estimates for drone point cloud using Equation 1.

Woodland type	Average AGB per tree (kg)	Total AGB (kg/ha)	Total C (kg/ha)	Total CO2 (kg/ha
Whole temperate forest	1176.43	777,697.68	281,993.18	1,034,914.97

Table 3. Tree metric values for NT Drone data, splitting point cloud into deciduous and coniferous.

Woodland type	No. Trees	Max crown area (m^2)	Average Crown Area (m^2)	Max tree height (m)	Average Tree Height (m)	Max crown perimeter (m)	Ave Crown Diameter (hull) ($m^)$	Max Crown diameter (hull) (m)
Temperate coniferous forests	596	312.97	29.76	23.96	1.72	62.75	17.66	62.75
Temperate deciduous forests	10,034	282.83	19.72	39.78	6.25	61.09	14.89	61.09
Whole temperate forest	10,577	312.97	20.42	39.78	11.83	67.74	15.09	62.74

9.2 Photographs taken of Home Covert Woodland

9.2.1 Home Covert at a distance


9.2.2 Pine Plantation Felling – Southern region of Home Covert



9.2.3 Ground data – Trees used for ground data measurements, in tree number order, including picture of tree, GPS coordinate and diameter breast height.






GPSmap 62
GARMIN
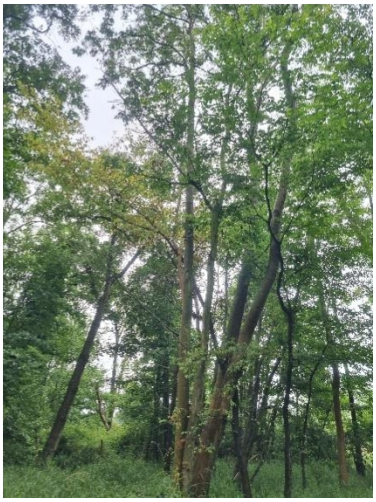


GPSmap 62
GARMIN



GPSmap 62
GARMIN




GPSmap 62
GARMIN

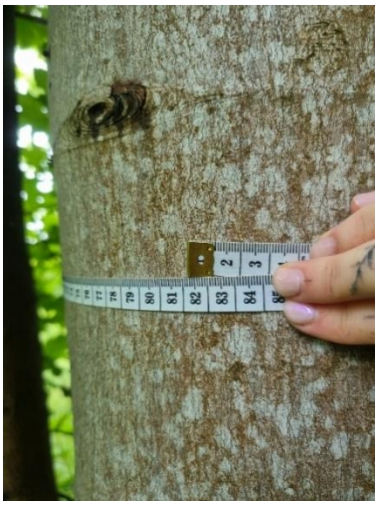

GPSmap 62
GARMIN



GPSmap 62
GARMIN




GPSmap 62
GARMIN



GARMIN



GARMIN